

1 **Advanced control strategies for bioprocess**  
2 **chromatography: challenges and opportunities for**  
3 **intensified processes and next generation products**

4 **Alexander Armstrong<sup>1,^</sup>, Kieran Horry<sup>1,^</sup>, Tingting Cui<sup>2</sup>, Martyn Hulley<sup>2</sup>, Richard**  
5 **Turner<sup>2</sup>, Suzanne S. Farid<sup>1</sup>, Stephen Goldrick<sup>1,\*</sup>, and Daniel G. Bracewell<sup>1,\*</sup>**

6 <sup>1</sup> The Advanced Centre of Biochemical Engineering, Department of Biochemical Engineering, University  
7 College London, Bernard Katz Building, Gower Street, London, WC1E 6BT, UK.

8 <sup>2</sup> Purification Process Sciences, Biopharmaceuticals Development, R&D, AstraZeneca, Cambridge, UK  
9

10 \* Correspondence: [d.bracewell@ucl.ac.uk](mailto:d.bracewell@ucl.ac.uk); Tel.: +44 (0) 20 7679 9580

11 Correspondence: [s.goldrick@ucl.ac.uk](mailto:s.goldrick@ucl.ac.uk)

12 <sup>^</sup> Both authors contributed equally to this work  
13

14 **Conflicts of Interest:** "The authors declare no conflict of interest."  
15

16 **Abstract**

17 Recent advances in process analytical technologies and modelling techniques present  
18 opportunities to improve industrial chromatography control strategies to enhance process  
19 robustness, increase productivity and move towards real-time release testing. This paper  
20 provides a critical overview of batch and continuous industrial chromatography control  
21 systems for therapeutic protein purification. Firstly, the limitations of conventional industrial  
22 fractionation control strategies using in-line UV spectroscopy and on-line HPLC are outlined.  
23 Following this, an evaluation of monitoring and control techniques showing promise within  
24 research, process development and manufacturing is provided. These novel control strategies  
25 combine rapid in-line data capture (e.g. NIR, MALS and variable pathlength UV) with  
26 enhanced process understanding obtained from mechanistic and empirical modelling  
27 techniques. Finally, a summary of the future states of industrial chromatography control  
28 systems is proposed, including strategies to control buffer formulation, product fractionation,  
29 column switching and column fouling. The implementation of these control systems improves  
30 process capabilities to fulfil product quality criteria as processes are scaled, transferred and  
31 operated, thus fast tracking the delivery of new medicines to market.

32 **Keywords:** process control, biopharmaceuticals, mechanistic modelling, process  
33 intensification, process analytical technology, real-time release testing

44 **1. Introduction**

45 The biopharmaceutical industry, currently dominated by therapeutic proteins, has grown  
46 rapidly since its inception while the portfolio of products has increased in complexity and  
47 diversity [1,2]. Concerns for the sector's future highlight rising development costs and  
48 manufacturing challenges, in addition to competition from biosimilars [3–5]. To ensure  
49 continual quality improvements and bring these complex therapeutic proteins faster to the  
50 market, companies have been driven to innovate by accelerating process development,  
51 reduce operational and capital expenses (OPEX and CAPEX), and move towards the goal of  
52 real-time release testing [6,7]. A key aspect in the manufacture of these therapeutic proteins  
53 is downstream processing where chromatography is typically the core purification technology  
54 [8]. Process optimisation and control of chromatography steps can contribute to more  
55 consistent product quality, better management of process variability, and cost reductions.  
56 However, the current implementation of chromatography control strategies in industry is  
57 limited and rudimentary, leading to processes operating sub-optimally in addition to delays in  
58 purification process development for new molecules. Therefore, a critical overview of the  
59 breadth of monitoring and control techniques is presented and possible future states of  
60 chromatography control that will pave the way towards greater process intensification are  
61 proposed.

62 The key questions that will be tackled in this review of current and future industrial  
63 chromatography control strategies are:

- 64 • What are the current standard buffer and fractionation control strategies in industrial  
65 chromatography?
- 66 • What novel process analytical technologies (PATs) and control strategies have been  
67 published?
- 68 • What are the benefits and issues of the novel PATs and control strategies described?
- 69 • What will be the likely future state of industrial therapeutic protein chromatography  
70 control systems to meet the challenges of increasing product complexity?

71 Process intensification was first pioneered as a way to reduce capital costs by the UK based  
72 Imperial Chemical Industries (ICI) in the late 1970s [9]. While it has since seen significant  
73 interest and application in the biopharmaceutical industry, the definition of process  
74 intensification has been vague and sometimes contradictory [10–13]. For the purposes of this  
75 review, process intensification is defined as any technology or strategy that increases the  
76 efficiency of one or more unit operations, leading to increased intermediate/final product purity  
77 and/or yield per unit volume, process time, and/or expense, resulting in reduced plant

78 footprints. In this manner, process intensification results in more efficient processes that meet  
79 regulatory requirements.

80 To tackle the growing expenses and demands of the biopharmaceutical industry, key  
81 regulatory agencies have pushed in recent decades to improve and modernise the  
82 biopharmaceutical industry. A key element of this is the “Quality by Design” (QbD) initiative,  
83 first developed by Dr. Joseph M. Juran [14]. QbD is an approach to development, based on  
84 quality planning, quality control, and quality improvements. Since its inception, it has been  
85 identified as a key design strategy by The International Council for Harmonisation of Technical  
86 Requirements for Pharmaceuticals for Human Use (ICH) guideline Q8, resulting in a  
87 continuous push by regulators for its implementation [15,16].

88 The QbD process requires the development of an overall control strategy, within which  
89 relevant critical quality attributes (CQAs) are identified along with their acceptable operating  
90 ranges [17]. The critical process parameters (CPPs) that directly impact the pertinent CQAs  
91 are also identified. A QbD control strategy can require monitoring of the CQAs and  
92 manipulation of the CPPs in response to the process changes to maintain the process within  
93 the established design space. Table 1 details potential CPPs, CQAs and performance  
94 attributes relevant to process chromatography for the purification of therapeutic proteins. The  
95 pertinent CQAs and CPPs are identified via risk assessment during process development, and  
96 vary depending on the chromatography process in question. For example, a Protein A capture  
97 step may have fewer and less-stringent CQAs than a polishing ion-exchange step where the  
98 product stream is nearing the final product composition. Performance attributes, such as  
99 product yield and process productivity, are not classed as CQAs as they do not directly affect  
100 the safety or efficacy of the final product. However, they remain vitally important to assuring a  
101 feasible manufacturing process, and so relevant process parameters influencing the  
102 performance attributes also require identification to enable their control [18,19].

103 Furthermore, the “Pharmaceutical Current Good Manufacturing Practices (cGMPs) for the  
104 21st Century—a Risk Based Approach,” is an initiative announced by the FDA in August of  
105 2002 to improve and modernise pharmaceutical manufacturing [20]. A vital element of the  
106 initiative is to encourage companies to adopt PAT for monitoring and control of processes,  
107 resulting in continuous real-time quality assurance. The utilisation of PAT plays a role in  
108 meeting the goals of the QbD design approach by monitoring the identified CQAs and  
109 manipulating the corresponding CPPs. For these reasons, a major focus in industry has been  
110 to improve the process efficiency and robustness of chromatography through the  
111 implementation of process monitoring and control using PAT.

112 However, while the ability of these PAT to monitor processes has been demonstrated in  
113 research and process development, the number of demonstrated implementations of control  
114 strategies utilising PAT is significantly lower [21–24]. This indicates a gap in meeting all the  
115 objectives of the FDA initiative. For industrial chromatography processes, these gaps exist  
116 due to the additional obstacles for PAT and process control implementation present in  
117 therapeutic protein chromatography when compared to small molecule chromatography. The  
118 first of these obstacles is the presence of product-related impurities including DNA and a  
119 variety of host cell proteins which must be reduced to nominal levels in the final product.  
120 Second, the similar binding affinities between the product and its aggregates, fragments, and  
121 dimers/monomers make their separation from the product challenging. Third, the difficulty in  
122 differentiating between product and product-related impurities using current PAT monitoring  
123 strategies means additional time and expenses are generated from retrospective off-line  
124 quality checks. Fourth, the wide variety of therapeutic proteins with different chemical  
125 compositions and configurations requires the development of individual control strategies for  
126 each product leading to long process development times [21–23].

127 These obstacles make accurate real-time measurements of therapeutic protein quantity and  
128 purity using traditional monitoring methods challenging. As a result, currently implemented  
129 chromatography control strategies in industry are relatively limited, reducing the process  
130 robustness and efficiency that can be achieved. Advanced control strategies could reduce  
131 expenses by decreasing buffer and material requirements, and intensifying chromatography  
132 steps resulting in processes with higher productivities that may lead to more robust processes  
133 with a smaller plant footprint.

134 Improved process control is also a key element in the move towards real-time release testing  
135 (RTRT) [25]. For biologics, RTRT is an alternative approach to standard product testing at the  
136 end of production, on the basis that the manufacturer can demonstrate that product quality is  
137 maintained based on real-time process data [26]. Strategies for the implementation of RTRT  
138 across biologic manufacturing can be found in the literature [25], and in published guidance  
139 from US and European pharmaceutical regulators [26–28]. The potential benefits of RTRT  
140 founded on advanced process control and PAT implementation include increased quality  
141 assurance, shorter production timelines, reduced OPEX and less dependence on  
142 retrospective end-product testing. These advanced systems require the use of multivariate  
143 data analysis (MVDA), mechanistic modelling, and in-line or automated on-line technologies  
144 to rapidly monitor and predict the process attributes in real time.

145 This review begins by highlighting the current buffer and fractionation control strategies used  
146 in industrial chromatography and identifies their limitations. This is followed by a deep dive

147 into literature for novel chromatography control strategies, starting with experimentally  
148 demonstrated spectroscopy-based soft sensors utilised in chromatography control strategies.  
149 The demonstrated and potential application of mechanistic modelling, PID controllers and  
150 model predictive control to industrial chromatography control are then further discussed,  
151 including the pros and cons of each strategy. Finally, a future perspective on advanced  
152 chromatography control systems and technologies is presented.

## 153 **2. Current industrial chromatography control systems**

154 The biopharmaceutical industry employs several monitoring and control technologies to  
155 ensure that chromatography systems operate safely, and that the product obtained meets the  
156 required specifications. In process chromatography there are two main areas for control:  
157 controlling the conditions of the column feed and controlling the purity and yield of the product.  
158 In this review, these areas are referred to as buffer control and fractionation control  
159 respectively. Currently available and industrially proven control technologies applied in both  
160 areas are detailed in the following two sections. A summary of the techniques discussed is  
161 provided in Table 2.

### 162 **2.1. Buffer control systems**

163 At industrial scale, protein purification can require thousands of litres of buffer weekly and a  
164 multitude of different buffer formulations per unit operation. In standard operation, buffers are  
165 formulated, tested and stored prior to consumption, often in large stainless steel tanks. Buffer  
166 formulation requires substantial resource and time, potentially involving off-line testing to  
167 ensure each buffer meets the required specification. It follows that buffer management  
168 contributes significantly to the overall plant footprint and can incur significant CAPEX and  
169 OPEX, with some authors citing buffer management as a prominent bottleneck in the entire  
170 production line [29]. As detailed in Table 2, two control techniques are readily available to  
171 address the buffer bottleneck, namely in-line dilution (ILD) and in-line conditioning (ILC).

172 Figure 1a details the ILD configuration which requires the preparation of concentrated buffer  
173 solutions, which are precisely diluted in-line using water for injection (WFI) [30]. The diluted  
174 buffer is then fed directly into the chromatography column. Most buffer solutions required for  
175 chromatography are relatively dilute. Therefore, storing highly concentrated versions and  
176 diluting in-line drastically reduces the size and quantity of buffer preparation and storage  
177 vessels required [31]. Cost savings are further enhanced if ILD reduces volume requirements  
178 to a point where single-use bags can be used instead of tanks. The ILD can be controlled by  
179 calculating the flowrate set-points of the concentrated buffer(s) and WFI streams prior to  
180 running the process. During ILD, flow indicators on each stream provide feedback to the  
181 controller, which manipulates the pumps and flow control valves to ensure the set-points are

182 met, as shown in Figure 1a. Secondary feedback can be facilitated using final buffer pH and  
183 conductivity readings if required [32], whilst accounting for potential probe drift and erroneous  
184 calibration. Flowmeters typically provide highly reliable data. However, when relying on flow  
185 control only, the pre-formulated buffer concentrates must be prepared with great precision as  
186 dilution will propagate any small errors introduced [31]. ILC eradicates this issue and can  
187 instigate further CAPEX and OPEX reductions.

188 ILC considers the controlled formulation of bioprocess buffers from individual component  
189 solutions and WFI immediately prior to consumption. The resulting buffer is fed directly into  
190 the purification process, thereby eliminating the need for laborious buffer formulation and  
191 storage prior to running the process. An example ILC system is provided in Figure 1b. The  
192 plant footprint and cost reductions can be greater than that of ILD, as individual buffer  
193 components can be stored in higher concentrations than a pre-formulated buffer concentrate  
194 [29]. Furthermore, any deviations in concentration, pH or conductivity from specification  
195 potentially introduced during dilution are prevented. A chromatography ILC system utilises  
196 four inlets namely: acid components, base components, salt solution, and WFI. As with ILD,  
197 feedback control is implemented to ensure that the final buffer solutions meet the  
198 specifications. If precisely formulated stock solutions of acid, base and salt are available,  
199 feedback control using only flowrate measurements and pre-determined flowrate set-points is  
200 possible (see Figure 1b). The conductivity and pH of the final buffer are monitored to ensure  
201 the product is suitable for real-time use. Dynamic feedback control using conductivity and pH  
202 probes is also possible and should be considered in situations where close control of the pH  
203 or conductivity is required, such as during linear gradient elution, or where variability in the  
204 stock solutions is anticipated.

205 The benefits of the ILD and ILC buffer control systems are numerous. For example, Kedrion  
206 Biopharma showed that implementing ILC reduced their tank requirements by 84%, facilitating  
207 the adoption of single-use buffer tanks [33]. Furthermore, the buffer preparation time was  
208 reduced by 69%, and the overall plant footprint was reduced by 61%. The benefits of  
209 automating buffer formulation by applying feedback control are clear: it reduces CAPEX and  
210 plant footprint, simplifies buffer preparation, and improves process robustness by reducing  
211 buffer variability. It follows that the implementation of in-line buffer formulation systems will  
212 become more commonplace, as control system expenses reduce and regulatory familiarity  
213 with the technology improves.

## 214 **2.2. Fractionation control systems**

215 A critical process control decision is selecting when to collect the product from the eluting  
216 stream. A typical product fractionation control system is depicted in control loop A of Figure 2.

217 The controller relies on in-line data from an ultraviolet (UV) spectrophotometer at the column  
218 outlet to inform the control decision. As detailed in Table 2, UV absorption at 280 nm is a well-  
219 established method for quantifying the total protein content during the process [34]. The UV  
220 280 nm absorbance is monitored continuously in-line, and the spectroscopy data is fed to the  
221 fractionation control unit. The control unit then dictates whether the column outlet stream is  
222 collected as product or is directed to waste. A common strategy employed is to instigate  
223 product collection when a minimum UV absorbance threshold is surpassed and terminate  
224 collection when the UV absorbance falls below a pre-determined value. The absorbance  
225 threshold used should be low enough to prevent significant product loss, but should ensure  
226 that product collection is not instigated too early due to inherent process disturbances or  
227 detector noise [35].

228 In analytical chromatography applications, defining the collection point is usually trivial; the  
229 eluting components are typically well resolved. However, this is not always the case for  
230 industrial systems. Productivity requirements mean industrial chromatography systems are  
231 often overloaded and therefore, component elution profiles overlap. This challenging  
232 purification scenario is demonstrated graphically in Figure 3a, where a product molecule elutes  
233 between early and late eluting impurities. Due to the presence of impurities before and after  
234 the product peak, it is not possible to start and stop product collection based on a minimum  
235 UV 280 nm absorbance threshold. Furthermore, the single wavelength absorbance data  
236 provides a surrogate measure of the total protein content and cannot be used to ascertain the  
237 relative amounts of different protein species in the eluent. Finally, high column loading also  
238 results in a wide range of protein concentrations at the column outlet, leading to saturation of  
239 the UV spectrophotometer. Therefore, selecting the optimum product collection times during  
240 an industrial scale multicomponent purification is a great challenge, especially when  
241 separating complex products from multiple product-related impurities.

242 To mitigate the risk of low product yield and high impurity content, product can be collected in  
243 discrete fractions spanning the width of the product elution peak. The individual fractions can  
244 then be analysed off-line, and the appropriate fractions pooled together to obtain a final pool  
245 that meets the specifications. However, under GMP regulations, retrospective off-line analysis  
246 adds an entire manufacturing shift to the production timeline, and incurs additional  
247 consumption of materials and resources [36]. Furthermore, the large volumetric flowrates  
248 observed during large-scale chromatography means collecting and analysing multiple eluate  
249 fractions is impractical. It follows that there is a substantial need to identify optimal product cut  
250 times during the chromatography process. To enable this, deconvolution of the chromatogram  
251 is required in real-time, so that the data can be transmitted to the fractionation controller during  
252 the process.

253 To obtain the additional data required to better-inform process control, on-line high-  
254 performance liquid chromatography (HPLC) systems positioned at the column outlet can be  
255 used (see Table 2). On-line HPLC is now finding regular application in industry, following  
256 several publications demonstrating the ability of automated HPLC systems to inform  
257 chromatography process control [36–38]. By introducing a fully automated sampling line from  
258 the column outlet, and feeding this into an analytical chromatography system, the large-scale  
259 chromatogram can be deconvoluted retrospectively. Data regarding separate co-eluting  
260 species is then passed to the control algorithm, enabling better-informed cut time selection.  
261 HPLC assays are robust and well-established, can handle broad concentration ranges, and  
262 can provide accurate concentration data to the controller. Furthermore, multiple columns can  
263 be operated in parallel to significantly reduce the delay between sample acquisition and data  
264 transmission to the controller.

265 However, the time associated with sampling and analysis still incurs a significant process  
266 delay, and on-line HPLC requires substantial CAPEX relative to UV-based fractionation. The  
267 requirement for an auto-sampler and potentially multiple HPLC units also increases system  
268 complexity. In addition, high-pressure (> 600 bar) HPLC is often utilised to enable shorter  
269 analysis times and provide data to the controller in shorter timeframes. Shorter HPLC elution  
270 times may result in peak overlap of similar proteins and so may not be able to give satisfactory  
271 resolution for complex separations [37]. Therefore, the addition of on-line HPLC is only  
272 recommended when there is a clear business case; the cost savings and process robustness  
273 improvements must outweigh the higher CAPEX and increased complexity on the  
274 manufacturing floor [36].

275 Additional process control challenges are introduced when operating a continuous  
276 chromatography system. Continuous chromatography makes use of multiple chromatography  
277 columns in series to utilise the full loading capacity of each column. It is generally used for  
278 'bind-and-elute' chromatography, with column operation consisting of the load, wash, elution,  
279 and regeneration steps. Many terms have been used to describe continuous chromatography.  
280 These include periodic counter current (PCC), simulated moving bed (SMB), and sequential  
281 multicolumn continuous chromatography (SMCC) [39–41]. These different continuous  
282 chromatography systems have different levels of complexity and flexibility, complicating the  
283 development of control systems for continuous chromatography. While utilising differing  
284 terminology, number of columns, and methods to explain and visualise the process, the  
285 underlying theory and mechanisms are the same. Multiple columns are used to run loading  
286 continuously and elution discretely in a cyclical fashion. An example of a continuous  
287 chromatography setup, which makes use of three columns in a continuous six-step cycle, has  
288 previously been described by Warikoo et al. [40]. Thus, for the purpose of demonstrating and

289 commenting on continuous chromatography control schemes in this review, a three-column  
290 process is considered (see Figure 4).

291 Continuous chromatography offers several distinct benefits when compared with traditional  
292 batch chromatography. First, the greater utilisation of the resin allows for similar processes to  
293 be operated with smaller columns when compared to batch. Second, the reduced column size  
294 reduces the amount of buffer needed, thus reducing CAPEX, OPEX, and can yield higher  
295 productivity [42–45]. However, industrial application of continuous chromatography is less  
296 common due to the increased operational complexity when compared to batch processes.  
297 This is evident in Figure 4, where an additional control loop (control loop B) and valve  
298 manifolds are required to facilitate column switching. Control loop B functions by utilising in-  
299 line UV 280 nm readings at the column flow-through outlet to direct the feed and buffer streams  
300 into the appropriate column. When the UV absorbance at the outlet of the second column  
301 surpasses a pre-determined breakthrough absorbance, the control unit manipulates valve  
302 positions in the inlet and outlet manifolds to move to the next step in the cyclic process outlined  
303 by Warikoo et al. [40]. The feed stream is directed to the inlet of column 2, the flow-through  
304 stream is redirected to column 3, and the fully-loaded column 1 is prepared for elution. The  
305 controller guides the process through the six-step cycle, mitigating product loss even as  
306 column binding capacity deteriorates and feed content varies. Traditionally, continuous  
307 chromatography is controlled through timed column switching based on pre-determine  
308 breakthrough times. However, this has the downside of not accounting for changes in feed or  
309 resin. This can result in lower column utilisation, product purity and yield, thereby  
310 demonstrating a key benefit associated with improved process control.

311 The increased complexity of continuous chromatography also introduces further product  
312 fractionation challenges in addition to those summarised for batch systems. When applying a  
313 timed column switching strategy, subtle variations in elution profiles and resin binding capacity  
314 can introduce column-to-column variability in purity and yield [46]. The impact of this variation  
315 is demonstrated in Figure 3b. Despite applying a constant product collection time,  $t_p$ , and time  
316 between column switches,  $t_{CS}$ , to each of the columns, the theoretical purity and yield of the  
317 product stream obtained from each column is different. In the second column, the product  
318 molecule elutes slightly later than expected, resulting in a reduction in purity and yield. In the  
319 third column, the quantity of product bound to the column is lower, potentially due to variations  
320 in the product concentration in the feed or column binding capacity, resulting in a lower product  
321 purity in the product stream. This further demonstrates the potential gains associated with an  
322 adaptive fractionation strategy that can respond to inherent process variation.

323 From the information presented, it is evident that the fractionation control technologies applied  
324 to batch and continuous chromatography are limited. In particular, product fractionation  
325 controllers are limited by the basic UV spectroscopy and time-consuming HPLC systems used  
326 to inform fractionation decisions. Consequently, alternative techniques have been developed  
327 to rapidly provide substantial product and impurity concentration data to the controller in real  
328 time, or predict the optimum product cut times in advance. More advanced process controllers,  
329 PID and model predictive control systems, also rely on real-time data to function effectively.

### 330 **3. Advanced monitoring and control technologies in research and process** 331 **development**

332 The most promising technologies for industrial chromatography control are spectroscopy  
333 instruments in conjunction with multivariate data analysis (MVDA), mechanistic modelling-  
334 based controllers and model predictive control. Therefore, a review of spectroscopy-based  
335 control strategies demonstrated in research and process development is given. This is  
336 followed by a summary of mechanistic modelling, PID control and model predictive control  
337 applied to industrial chromatography control systems.

#### 338 **3.1. Spectroscopy-based control systems**

339 Although the majority of published chromatography research typically focuses on process  
340 monitoring, there has been a recent increase in applications that demonstrate process control  
341 which are summarised in Table 3. Due to rapid measurement time and relatively high  
342 accuracy, recent advanced chromatography control strategies primarily utilise spectroscopy-  
343 based PAT for in-line monitoring of the process. While UV 280 nm spectroscopy remains the  
344 dominant spectroscopy tool for process monitoring and control, there are now several other  
345 spectroscopy PATs available. These include infrared (IR), Raman, multi-angle light scattering  
346 (MALS), variable pathlength UV, fluorescence, and combined multi-sensor systems. The  
347 spectroscopy data generated by these PATs can be correlated to specific CPPs or CQAs  
348 through the development of MVDA or machine learning models and can provide real-time  
349 predictions of these variables. These predicted CQA or CPP measurements are often classed  
350 as “soft-sensors” and can be integrated within a controller to enhance their monitoring and/or  
351 control [47–49]. A review of these spectroscopy PATs implemented within process control  
352 strategies is discussed.

353 PAT often requires the application of multivariate data analysis (MVDA) and machine learning  
354 methods to extract useful information from large quantities of multivariate raw data [34]. The  
355 need for MVDA techniques is especially prominent for spectroscopy-based PATs, due to the  
356 potentially large number of variables (wavelengths) and typically noisy signals captured. The  
357 results of MVDA can be used to make predictions of product CQAs, and inform process control

358 decisions. Two MVDA techniques frequently applied to spectra are principal component  
359 analysis (PCA) and partial least squares (PLS) regression [21]. In PAT applications, PCA is  
360 well-suited to detecting and enabling removal of erroneous data points in multivariate datasets  
361 responsible for an unexpected increase in variance [50,51]. Whilst PCA can also be extended  
362 to make predictions of product CQAs via principal component regression [52], PLS is the  
363 prevalent regression technique applied to predict attributes from spectroscopy data. Methods  
364 for constructing and optimising PCA and PLS models can be found in the comprehensive  
365 review by Rolinger et al. [21], and elsewhere in the literature [52–55].

### 366 **3.1.1. UV/vis spectroscopy**

367 Due to its common usage in industry, UV spectroscopy has seen more focused interest as a  
368 PAT in the development of process control strategies for chromatography. The simplest UV  
369 spectroscopy control methods utilise a single wavelength. The monitoring method measures  
370 the difference between the breakthroughs UV versus the feed, subtracting the baseline  
371 absorbance from both. There has been previous implementation of single wavelength UV  
372 spectroscopy to continuous chromatography [40,56,57]. In addition to controlling fractioning  
373 and loading decisions, the control strategies use the loading information to control column  
374 switching. This allows the process to switch columns at the optimal time based on changes to  
375 the feed, which timed-column switching cannot accomplish in real-time, as outlined in Figure  
376 3. However, single wavelength controllers have limited accuracy when compared to more  
377 complex spectra controllers.

378 In order to improve the accuracy of the PAT, the UV/vis absorbance of a solution over a  
379 spectral range can be measured [58,59]. This is due different amino acids absorbing different  
380 amount of light at different wavelengths, giving each protein its own spectral fingerprint.  
381 Utilising this spectra fingerprint, it is possible to differentiate and quantify proteins within a  
382 multi-protein solution. Multi-wavelength UV/vis spectroscopy monitoring methods has seen  
383 the application in the control of fractioning and pooling of batch protein A chromatography [60].  
384 Using a spectral range of 200 to 410 nm, a PLS model was calibrated and validated for the  
385 differentiation of protein and impurities. The PLS model was then applied to the real-time  
386 monitoring of the varying protein concentrations. By utilising a broad spectral range rather than  
387 a single wavelength, the control strategy was able to accurately differentiate product and  
388 impurities when compared the traditional single-wavelength counterparts. The final model,  
389 which subtracted the impurity background, reached a root mean squared error (RMSE) of 0.01  
390 mg/ml for predictions and, it showed promise for the application to continuous chromatography  
391 as well. However, while the use of a PLS model for the monitoring and control of the process  
392 shows promise, it does come with drawbacks. First, the PLS model was difficult to accurately  
393 calibrate over a wide range of concentrations, making high feed concentration variability of

394 problem for the control strategy. Second, high feed concentrations may lead to saturation of  
395 the detector, preventing the PAT from accurately informing the model. Finally, as the number  
396 of impurities present in the feed increases, the accuracy of the model decreases [59].

397 Finally, mechanistic control models coupled with UV spectroscopy monitoring has seen  
398 implementation in a two column continuous chromatography control [61]. The work utilizes a  
399 transport dispersive mechanistic model-based approach to design, optimise and control the  
400 process. By measuring the concentration of the feed at-line with the use of a UV  
401 spectrophotometer, the model predicts when the product peak will elute and make the  
402 fractioning decision. In addition, the model accounts for aging resin (by reducing the density  
403 of the Protein A ligands parameter in the model) and changing upstream conditions. The  
404 implementation of the mechanistic controller successfully accounted for variations in the feed  
405 and the two column continuous chromatography set-up lead to a 2.5-fold higher capacity  
406 utilisation. The mechanistic model utilized for chromatography control in the paper is further  
407 discussed in section 3.2. While the mechanistic model does account for resin aging and  
408 varying upstream conditions, it does not capture all variability present in the system. This can  
409 lead to the mechanistic control method improperly determining the elution cutting times. A  
410 potential solution to this could be the implementation of an MVDA controller at the outlet to  
411 identify variations between the predicted and real output. Furthermore, the feed  
412 concentrations used were lower than typically seen in industry (0.2-0.8 g/L). For these  
413 reasons, further studies at large scale and higher feed concentrations are requirement to  
414 optimise this control strategy.

### 415 **3.1.2. Infrared (IR) spectroscopy**

416 Recently, through the implementation of multi-wavelength near IR spectroscopy (NIR)  
417 monitoring, the development of a control strategy for column load in continuous  
418 chromatography with Protein A columns has been demonstrated [62]. Initially a NIR flow cell  
419 was placed at the inlet of the columns and a spectrum of the feed was collected every 3  
420 seconds. Using a PLS model calibrated with a reference spectrum, the concentration of the  
421 mAb of interest could be determined to within  $\pm 0.05$  mg/ml. The control strategy utilized the  
422 information from the PLS model to ensure the feed concentration was between the desired  
423 operating range of 3 mg/ml to 8 mg/ml, ensured optimum resin utilisation, and controlled  
424 column switching and fractionation. The control strategy was designed to handle extreme  
425 deviations in feed concentration outside the desired operating range and adjust times in  
426 various steps of the continuous counter-current chromatography as needed. Through the  
427 implementation of a secondary NIR flow cell at the outlet, further insight is gained by  
428 monitoring changes in column binding capacity in real time. This provides early warning of  
429 resin degradation as well as other column issues. This system reduces resin cost while

430 increasing process predictability and consistency. The accuracy of Multi-wavelength NIR  
431 monitoring in real time was shown to be significantly better than multi-wavelength UV-  
432 spectroscopy, making it a more promising PAT for chromatography control. However,  
433 industrial scale tests are still required to fully verify and optimise the control method.

434 In addition to its ability to differentiate and quantify proteins and their impurities, IR  
435 spectroscopy has demonstrated potential application as a PAT for column fouling monitoring  
436 [63]. However, since water is strongly absorbed with the mid-IR light range, the transmission  
437 cell path length can be no more than a single layer of resin beads [64]. To overcome the path  
438 length limitation, Attenuated total reflection Fourier transform IR (ATR-FTIR) was utilised. ATR  
439 only probes a layer a few micrometres deep that is adjacent to the surface of the ATR crystal.  
440 With this technique, resin beads are fed into an in-column ATR-FTIR cell. The analysis  
441 methods is able to differentiate the beads, proteins, DNA, and lipids present in the column,  
442 providing the opportunity to characterise what component are primarily responsible for the  
443 column fouling. This provides more information on the state of the column than fluorescence  
444 spectroscopy does when it is applied to column fouling determination [65,66]. Though recent  
445 studies indicate that fluorescence spectroscopy may be simpler and more accurate to  
446 implement for real-time monitoring than ATR-FTIR, it is still a promising PAT due to its ability  
447 to differentiate product and impurities. Furthermore, scale-up studies are still required to  
448 confirm the findings on industrial scale.

### 449 **3.1.3. Raman spectroscopy**

450 A spectroscopic technique receiving increasing interest in literature due to its high molecular  
451 specificity, robustness and minimal water interference is Raman spectroscopy [67]. Raman  
452 and IR spectroscopy are both vibrational spectroscopy techniques that operate in the visible  
453 and near infrared region. Although no current literature has been published using Raman  
454 spectroscopy as a PAT in process control of chromatography, Raman spectrometry has seen  
455 recent interest as a PAT for monitoring chromatographic operations [68,69].

456 Raman spectroscopy has broad application in biology, chemistry and has been applied in  
457 many environmental and industrial applications [70]. This includes the identification of  
458 modified nucleosides, a tumour biomarker present in urine, for cancer diagnosis. Following  
459 separation using affinity chromatography, the modified nucleosides were supplemented with  
460 gold, and surface-enhanced Raman scattering (SERS) spectroscopy was utilised to create a  
461 biochemical profile of the markers [71]. Due to its ability to identify proteins as well as their  
462 aggregates, it has seen recent application to chromatography application. Raman  
463 spectroscopy has been used to quantify aggregation in 3 insulin analogues: lipro, aspart, and  
464 glulisine, highlighting its implementation as a PAT for aggregation determination [72].

465 Furthermore, Raman spectroscopy has been implemented as an on-line sensor to monitor  
466 breakthrough curves using an extended Kalman filter approach (EKF) analyser [69].  
467 Enhanced Raman spectroscopy techniques, such as UV resonance Raman spectroscopy  
468 (UVRRS), have been developed to increase sensitivity and minimise fluorescent interference  
469 [68]. Finally, Raman has seen application both upstream, as an at-line monitoring tool for high-  
470 throughput (HT) micro-bioreactor cultivation of mammalian cells, and downstream, to compare  
471 different elution conditions for a cation exchange (CEX) chromatography step for an Fc-fusion  
472 protein [54].

473 However, Raman spectroscopy does come with its drawbacks. First, the novel filters and  
474 lasers required are expensive and complex, as such its implementation outside of process  
475 development environments has been slow. Second, while conventional Raman spectroscopy  
476 has been proven at high protein concentrations, it is less robust and sensitive for lower  
477 concentrations. While Raman was able to measure protein concentration and monomer purity  
478 in CEX chromatography, it could not accurately predict of high and low molecular weight  
479 species, which were present in low concentrations [54]. Third, Raman scattering is inherently  
480 weak and is susceptible to fluorescent interference. When performing ion exchange  
481 chromatography on simulated plasma protein containing albumin and fibrinogen, the poorly  
482 soluble fibrinogen fraction caused significant impediment to the accuracy of the Raman spec  
483 analysis through [73]. This highlights the potential problems of implementing Raman  
484 spectroscopy as a PAT for chromatography control. The instrumentation costs are significantly  
485 more than that of the alternatives and problematic fluorescence can limit its application in  
486 biological samples. Despite this, it is evident that Raman spectroscopy has the potential to be  
487 used as a PAT analyser for chromatography; providing that core instrumentation costs fall,  
488 equipment familiarity improves and techniques such as UVRRS mature [67].

#### 489 **3.1.4. Light scattering technologies**

490 Light scattering technologies can be subdivided into two types. The first is static light scattering  
491 (SLS), which measures the light scattered at many different angles to determine the average  
492 intensity of a sample. This is useful to determine the structural characteristics of the sample.  
493 The second, dynamic light scatter (DLS), measures the fluctuations in the scattering intensity  
494 over time to characterise the diffusion of particles within a sample [74]. One promising SLS  
495 technology for chromatography monitoring is (MALS). Due to MALS ability to rapidly measure  
496 molecular weight in real time, it is a powerful tool to control for aggregate levels in product  
497 fractions. MALS can be used as a PAT on its own or combined with size-exclusion (SEC)  
498 chromatography [75]. In fact, MALS has seen recent implementation as an in-line PAT and  
499 on-line when coupled with ultra-high performance SEC chromatography (UHP-SEC- $\mu$ MALS)  
500 for the control of chromatography fractionation [76]. The rapid (<1s) MALS measurements

501 were able to reduce and control aggregate levels during fractionation, potentially removing the  
502 need for post purification analysis of aggregates. However, MALS is limited by two main  
503 drawbacks. First, rapid changes in concentration may affect the accuracy of MALS  
504 measurements. Second, MALS may be challenging to implement in other unit operations with  
505 significant difference in matrices and buffer conductivities [22]. For example, with bind-and-  
506 elute chromatography. Despite these hurdles, MALS remains a promising tool for fractionation  
507 control for chromatography process providing aggregate clearance.

### 508 **3.1.5. Variable pathlength UV-vis spectroscopy**

509 Industrial scale chromatography produces complex multicomponent outlet streams, often  
510 containing a wide range of protein concentrations. Therefore, protein concentrations observed  
511 are often outside the narrow linear range of standard UV/vis spectroscopy equipment. To  
512 overcome this challenge, UV/vis equipment has been developed that automatically changes  
513 the optical pathlength during process measurements, thereby extending the concentration  
514 range over which accurate measurements can be obtained, rendering sample dilution  
515 unnecessary [22].

516 Recently, two variable pathlength UV spectroscopy products have entered the market, namely  
517 the SoloVPE<sup>®</sup> and FlowVPE<sup>®</sup>. The FlowVPE<sup>®</sup> is of particular interest for process control, as it  
518 can be utilised in-line. The technology measures the UV absorbance of a solution at several  
519 pathlengths for each wavelength desired. For a given wavelength, a simple linear regression  
520 between the absorbance and the optical pathlength is assumed, and a least squares problem  
521 is solved to obtain the gradient and intercept. The gradient obtained is the critical component,  
522 as it is used together with the Beer-Lambert law to calculate the protein concentration in the  
523 solution [77]. This value can then be used to make better-informed control decisions, utilising  
524 only in-line equipment.

525 Despite the improvements stated, variable pathlength UV equipment maintains a key  
526 disadvantage from its fixed pathlength predecessor; the FlowVPE<sup>®</sup> is incapable of  
527 distinguishing between different proteins and their derivatives [22]. To overcome this, Brestrich  
528 et al. [77] applied MVDA to exploit the difference in absorbance spectra between different  
529 protein variants in a cation exchange chromatography effluent stream. A PLS model was  
530 developed, validated and utilised together with the in-line FlowVPE<sup>®</sup> to dictate product pooling.  
531 The variable pathlength UV equipment enabled measurements over a wide concentration  
532 range (<80 g/L), whilst the PLS model enabled differentiation between the protein species  
533 investigated. However, the system demonstrated was not without its own set of challenges.  
534 Differences in UV absorbance spectra between mAbs, high molecular weight and low  
535 molecular weight variants are subtle. Exploiting these differences presents a significant

536 obstacle to overcome via PLS modelling [77]. Additionally, the FlowVPE<sup>®</sup> still suffers from the  
537 inherent light scattering challenges associated with standard UV spectroscopy when  
538 quantifying highly concentrated, and therefore highly turbid, protein product streams [22].  
539 Furthermore, despite being an in-line technology, the measurement time was large (~30s)  
540 relative to standard spectroscopy equipment. This is due the requirement to adjust the location  
541 of the optical fibre for each pathlength measured [77]. It follows that further proof of method  
542 robustness, and optimisation of the variable pathlength UV spectroscopy acquisition and  
543 analysis times, would be of great interest to the field.

#### 544 **3.1.6. Fluorescence Spectroscopy**

545 While most PAT applied in chromatography are utilized in the control of fractionation and  
546 loading time, tryptophan fluorescence spectroscopy has been utilised for monitoring fouling  
547 and protein misfolding. The technology takes advantage of the fluorescence signal generated  
548 by tryptophan when excited by a 280 nm UV light source which can be measured in the 350  
549 nm range. This phenomenon was first applied to proteins in 1978, when tryptophan  
550 accessibility was used to differentiate the monomer and dimer of bovine aspartate  
551 aminotransferase, and has since been used to investigate a variety of protein structural  
552 changes [78–81]. Due to the utilisation of 280 nm light for excitation, the protein absorbance  
553 can be determined concurrently to misfolded proteins levels, thus making it a potential dual  
554 PAT in one. The Vernier Fluorescence/UV-VIS Spectrophotometer is an already existing tool  
555 that is able to achieve this.

556 Apart from misfolded protein determination, tryptophan fluorescence spectroscopy has shown  
557 promise for implementation as a PAT tool for screening a variety of cleaning in place (CIP)  
558 protocols for protein A chromatography. Many PAT have been tested as qualitative or  
559 quantitative analytical tools for fouling. These include HPLC, scanning electron microscope  
560 (SEM), mass spectrometry (MS), and Fourier transform infrared spectroscopy (FTIR).  
561 However, tryptophan fluorescence spectroscopy has been demonstrated to be superior in  
562 fouling determination as well as for screening a variety of cleaning in place (CIP) protocols  
563 for protein A chromatography [65]. In addition, the fluorescence-based PAT was applied for  
564 on-line monitoring and combined with control strategies to determine when to initiate column  
565 cleaning [66]. While not directly improving product purity and yields, the implementation of  
566 fluorescence spectroscopy reduces OPEX. The application of fluorescence spectroscopy as  
567 a PAT for CIP buffer screening has been shown to optimize CIP buffer to maximize foulant  
568 clearance while minimizing ligand degradation. This has the added benefit of improving  
569 column life span. Column fouling monitoring also serves to increase column life span and  
570 buffer utilisation. Rather than arbitrarily performing CIP after a set number of cycle, the control  
571 strategy determines when fouling has reached critical levels. This reduces the frequency of

572 CIP to only when the process requires it, reducing OPEX and increasing column lifespan. The  
573 variety of applications for the PAT make it a promising tool for chromatography control.  
574 However, fluorescence spectroscopy is limited due to utilising only one wavelength to measure  
575 tryptophan fluorescence, limiting the PAT's accuracy and ability to differentiate proteins.

### 576 **3.1.7. Multi-sensor systems**

577 The majority of spectroscopy-based PAT control systems proposed for industrial  
578 chromatography apply a single spectroscopy technique. Each system has associated benefits  
579 and shortfalls. To mitigate for these shortfalls, recent publications have explored multi-sensor  
580 systems, where data from several sensors is combined and leveraged to develop predictive  
581 empirical models [82,83]. The model outputs are then used to inform control decisions.

582 Sauer et al. [82] considered a cation exchange chromatography system for purification of an  
583 *Escherichia coli* derived growth factor, whereas Walch et al. [83] considered a Protein A step.  
584 The control systems proposed in both publications required the development a PLS model for  
585 each attribute tested. Sauer et al. [82] proposed three model categories; 1. basic models using  
586 standard UV, pH and conductivity signals; 2. medium models incorporating MALS and  
587 refractive index (RI) predictors; and 3. extensive models including ATR-FTIR and fluorescence  
588 spectroscopy techniques. All three model types were tested for each attribute, and the  
589 appropriate model in each case was determined using the root-mean squared error (RMSE).  
590 A significant reduction in RMSE would justify the application of a more complex model. For  
591 attributes where the extensive and medium models resulted in no significant reduction in  
592 RMSE, basic models were proposed.

593 In both papers, basic models were sufficient for overall quantity predictions, and extensive  
594 models were deemed appropriate for host-cell proteins and double-stranded DNA content.  
595 Walch et al. [83] required fluorescence, UV and RI signals for monomer content. ATR-FTIR,  
596 UV, RI and fluorescence signals best predicted high molecular weight impurity content. The  
597 developed models facilitated the application of model-based pooling strategies. Pooling  
598 criteria were based on maximum impurity content and minimum product content. The PAT  
599 control schemes designed compared well to equivalent at-line pooling schemes using the  
600 same pooling criteria.

601 However, the recent and comprehensive spectroscopy PAT review paper by Rolinger, Rüdts  
602 and Hubbuch [21] highlighted several factors that must be considered when deriving MVDA  
603 models from multiple sensor inputs. The main considerations highlighted are as follows.  
604 Firstly, when predicting DNA and HCP content, the output variables are typically ratios not  
605 linearly correlated to spectra and span several orders of magnitude. Therefore, nonlinear  
606 empirical modelling alternatives may be more suitable than linear modelling such as PLS.

607 Alternatively, nonlinear relationships could be accounted for during model building by including  
608 bivariate interaction and polynomial terms. Secondly, if multiple variables and several  
609 nonlinear terms are included in model building, it is critical that the empirical model does not  
610 succumb to overfitting or derive fictitious correlations. Thus, it is key that cross-validation  
611 functions are applied and that the number of samples is sufficiently large relative to the number  
612 of input variables. Finally, system complexity increases significantly when using multiple  
613 devices potentially with different sampling rates, analysis times and locations on a given  
614 process stream. It follows that data pre-processing and alignment is key to ensure subsequent  
615 analysis derives the correct outputs [21].

### 616 **3.2. Mechanistic modelling for chromatography control**

617 Mechanistic chromatography models are formulated from mathematical equations describing  
618 the mass transfer and adsorption phenomena observed during a chromatography separation  
619 [84]. Also referred to as first-principle models, they can provide more accurate and wider-  
620 ranging predictions than empirical modelling alternatives [85], and their value for industrial  
621 bioprocess design and optimisation is forecast to increase [86]. Mechanistic modelling of  
622 chromatography processes for process optimisation and robustness studies is a prevalent  
623 area of research [87,88]. However, with first-principle modelling accuracy and the efficiency of  
624 mathematical solvers improving, mechanistic models are finding a growing number of  
625 applications for chromatography process control for biopharmaceutical products [89].

626 For well-predicted systems, Kumar and Rathore [90] demonstrated that mechanistic model  
627 simulations conducted prior to running the separation can be used to dictate fractionation. This  
628 feedforward control strategy was dependent on the availability of feed composition data, which  
629 in this case was obtained using UPLC. In an industrial setting however, feed data may be  
630 readily accessible from the upstream operation. A more computationally efficient fractionation  
631 method using mechanistic model simulations of the product profile only and an in-line UV  
632 signal was also demonstrated [90]. The difference between the overall UV signal and the  
633 mechanistic model prediction of the product profile was used as a measure of the impurity  
634 content. This overcomes a well-known challenge associated with mechanistic modelling;  
635 adsorption modelling of heterogeneous impurity groups is a complex task [19]. The main issue  
636 identified with this method was the limited linear range of the UV signal. To accurately identify  
637 optimum start and end cut times using the UV signal and the predicted product profile, the  
638 chromatogram must be within the linear range of the UV detector.

639 Steinebach et al. [61] proposed also using the results of previously conducted mechanistic  
640 model simulations to inform continuous chromatography control actions, in the form of a look-  
641 up table. The constructed table could then be used to select a feed volume per cycle that

642 guarantees the required product yield for a given feed concentration and flowrate, whilst  
643 minimising buffer consumption and maximising capacity utilisation. However, identifying this  
644 optimum feed volume per cycle requires measurement of the feed concentration in real-time.  
645 As discussed in section 3.1, this can be challenging for concentrated multicomponent feed  
646 streams.

647 Westerberg et al. [91] demonstrated several theoretical mechanistic model-based cut  
648 strategies derived from an extensive sensitivity analysis. For an open-loop control system, a  
649 worst case UV absorbance value was calculated using an ideal fractionation strategy. This  
650 value was used as the absorbance threshold to trigger product collection for 200 subsequent  
651 mechanistic model simulations with process disturbances. Feed-forward control methods  
652 were also established by fitting linear functions to predict product cut time UV absorbance  
653 from several parameters. For example, a piecewise linear function was used to predict cut  
654 point absorbance from the load buffer conductivity. A relationship between the cut time UV  
655 absorbance and load buffer conductivity was observed during the preliminary sensitivity  
656 analysis.

657 In a more recent in-silico study, Borg et al. [35] demonstrated that, when the product molecule  
658 elutes before the impurities, identification of the first cut point is trivial and can be made based  
659 on the UV 280 nm absorbance threshold. However, identifying the second cut point required  
660 extensive in-silico investigation of the impact on product yield and purity. Robust product  
661 fractionation was obtained by selecting the cut point that gives a 99.5% probability of obtaining  
662 the target purity. To confirm the strategy, Borg et al. [35] conducted a further 100,000  
663 mechanistic model simulations with process disturbances, of which 99.6% obtained the target  
664 purity. Sreedhar et al. [92] applied and contrasted three different algorithms to identify optimal  
665 cut-times using empirical and mechanistic modelling, where the product of interest eluted as  
666 an intermediate. The mechanistic model was used to simulate an overloaded asymmetrical  
667 chromatogram on which to test the algorithms, whereas the empirical model was limited to  
668 generating simple symmetrical chromatograms. This demonstrates the enhanced ability of  
669 mechanistic modelling to capture the complexity of industrial scale chromatography relative to  
670 statistical alternatives.

671 Mechanistic model-informed process control has also been applied to chromatography  
672 processes integrated into a small-scale continuous end-to-end mAb production process [93].  
673 Mechanistic models were developed for each chromatography step in the purification train,  
674 and were used to build a comprehensive model of the entire downstream process. Following  
675 this, mechanistic model simulations were conducted during the real process to inform control  
676 decisions critical to the immediate chromatography cycle. For the product capture step, a

677 loading factor control strategy was implemented to maximise resin utilisation and mitigate  
678 product loss despite variable flow and concentration outputs from the bioreactor. Upstream  
679 production rates and concentrations were used in conjunction with the mechanistic model-  
680 derived DBC (at 1% breakthrough) to determine the load volume for a given cycle. The  
681 controller enabled consistent and higher product concentrations in the capture step product  
682 stream, and meant fewer cycles were required per process run thereby increasing column  
683 longevity. A feedforward control strategy was implemented to control fractionation in the  
684 subsequent ion-exchange steps. The mechanistic models were used to generate  
685 chromatograms during the process, utilising product loading data obtained from the complete  
686 downstream process model. Using the predicted peaks, theoretical UV absorbance cut-points  
687 were calculated that ensured sufficient impurity removal, and were subsequently applied to  
688 the real process. Therefore, the process was able to respond to variations in mAb  
689 concentrations and feed flowrates, and maintain the output within specifications. Both control  
690 schemes were proven over an extended period of 15 days. However, the continuous mAb  
691 production process was small-scale ( $0.8 \text{ mg ml}^{-1} \text{ day}^{-1}$  production rate using a 200 ml perfusion  
692 bioreactor), and demonstration of the control strategies at larger-scale is required. When  
693 purifying high-titre feed streams, reliance on a UV absorbance-based fractionation strategy  
694 may be infeasible due to the wide-ranging protein concentrations.

695 The benefits of using mechanistic models for control scheme design and testing is evident  
696 from the examples given. By working in silico, a multitude of operating conditions and  
697 fractionation strategies can be trialled rapidly with minimal expenses and negligible material  
698 consumption prior to running the real process [35,61,91,92]. Alternatively, by utilising the  
699 mechanistic model in real-time in a feedforward configuration, the need for real-time feedback  
700 to the controller is eliminated thereby facilitating real-time control decisions. However,  
701 mechanistic model-based strategies are not without their drawbacks. Firstly, such control  
702 schemes are reliant on having a readily available and validated mechanistic model of the  
703 large-scale process. Whilst this is not typically the case in industry today, recent publications  
704 highlight the need to encourage industry uptake of mechanistic models and provide potential  
705 solutions to the uptake issue. Potential solutions include providing freely available open-  
706 source mechanistic modelling software [94], standardising the model development process  
707 [95], and introducing a methodology for quantifying the predictive ability of a mechanistic  
708 model [96]. Secondly, feedforward controllers are heavily reliant on the accuracy of the  
709 process model utilised, and are unable to respond to unpredicted process deviations.  
710 Therefore, feedback control loops utilising well-established control techniques able to respond  
711 to such deviations, such as PID and MPC controllers, may provide more robust control  
712 alternatives.

### 713 3.3. PID controllers for product fractionation

714 Proportional-integral-derivative (PID) control is a well-established and simple feedback control  
715 technique applied routinely throughout industry. The controller output is calculated in response  
716 to the error from a given process set-point, using three modes of control; proportional (P),  
717 integral (I) and derivative (D). Theoretically, the modes can be applied individually or  
718 collectively. However, PI controllers are the most commonly used, followed by simple P and  
719 full PID controllers [97]. Once the PID control parameters are tuned (using techniques such  
720 as the Ziegler-Nichols method) a PID control algorithm can mitigate deviations from set-points  
721 with negligible overshoot and lag. Furthermore, the controller can also be used to facilitate a  
722 controlled change in process set-point.

723 Within bioprocesses, a PID controller is typically applied to regulate easily monitored variables  
724 such as temperature, flowrates and pH. Furthermore, the output from more advanced  
725 controllers, such as MPCs, may adjust the set-point of several simple PID control loops,  
726 thereby relying on the PID controller to implement the required changes. Within  
727 biochromatography, PID controllers have been used to control product purity and identify  
728 optimum cut-times [98,99].

729 In the first example, a PID controller was designed and applied to two purification processes,  
730 using standard UV 280 nm signals to provide feedback data to the control system [99]. The  
731 objective of the controller was to ensure the product peak was positioned at a predetermined  
732 optimum location within the product elution window. PID control relies on a single input.  
733 Therefore, the UV signals obtained were converted to a single value via two alternative  
734 techniques, which were later compared. The simple peak maximum method determined the  
735 time at which the UV peak maximum occurred, and fed this value to the PID controller. The  
736 second approach accounted for the non-Gaussian shape of an overloaded industrial  
737 chromatogram. The chromatogram was integrated, and the first moment of the chromatogram  
738 area in the  $x$ -axis (time) was computed and fed to the control scheme. The PID controller then  
739 adjusted the cut-time to minimise the error between the time value calculated and the set-point  
740 time. The results showed that the PID controller was able to move the collection window to  
741 the desired point and handle process disturbances, using only a UV 280 nm signal. However,  
742 the basic nature of the UV signal meant it was not possible to track product yield and purities  
743 during the process.

744 In the second publication, an at-line HPLC system was used to provide information to a PID  
745 controller for a two column mAb purification [98]. The product molecule eluted as an  
746 intermediate. Therefore, two PID controllers were employed; one to control the early eluting  
747 impurity content and another to control the late eluting impurity content. Both PID controllers

748 were tuned in silico prior to experimentation, using a mechanistic model derived in a previous  
749 publication [100]. The PID controllers were then employed as follows. Firstly, the product outlet  
750 stream was analysed via HPLC during the cycle. Thus, a deconvoluted chromatogram was  
751 available prior to the next cycle. The resulting chromatogram was then integrated using the  
752 trapezium rule. The difference between the calculated impurities content and a pre-determined  
753 set-point was fed to the PID controllers as an error. The two PID controllers then calculated  
754 the start and end salt concentrations for the product elution window. Finally, the required  
755 control action was computed via mass balance using the output salt concentrations. The  
756 controller was proven in two lab applications, firstly using a synthetic three-protein feed, and  
757 secondly with a clarified cell culture supernatant. In both cases, the PID controllers reduced  
758 the error to negligible levels within 5 cycles and were able to handle disturbances in flowrate  
759 and feed concentration. The controllers also automated the complex task of setting the recycle  
760 rate during start-up. However, the target impurity content (5%) was less-challenging than a  
761 typical industrial system, and the significant delay associated with at-line HPLC meant real-  
762 time control decisions were not feasible. Furthermore, at-line sampling required operator  
763 intervention and removal of product from the process, highlighting the requirement for  
764 advanced PATs to rapidly provide composite data to the control scheme.

765 Both the UV and HPLC-based systems tested demonstrate that closed-loop PID controllers  
766 can be used to determine product cut-times during the process, thereby ensuring consistent  
767 attainment of the product quality attributes despite uncontrolled disturbance and variable feed  
768 compositions. However, for PID controllers to provide real-time control actions, detailed  
769 information regarding outlet compositions is required rapidly. As discussed previously, this is  
770 a great challenge for biomolecules. Furthermore, PID controllers require testing and tuning  
771 prior to application. This is relatively trivial and can be conducted in silico if an accurate  
772 mechanistic model of the process is readily available. Alternatively, if the purification process  
773 is similar to that demonstrated by Krättli et al. [98,99], the PID parameters provided may be  
774 suitable as a starting point. If no such model is available, substantial quantities of materials  
775 and time may be required to tune the controller. Finally, PID control schemes are relatively  
776 basic. Whilst this may enable cheap and simple implementation, more advanced control  
777 schemes (such as model predictive control) may be able to provide more accurate feedback  
778 and critically, they can facilitate process optimisation during production.

### 779 **3.4. Model predictive control**

780 Model predictive control (MPC) is a powerful control strategy developed to control multivariate  
781 non-linear systems where simple alternatives, such as PID controllers, are insufficient [101].  
782 The benefits of MPC over alternative control methods are numerous [102]. MPC schemes are  
783 able to deal with a large number of manipulated and controlled variables, incorporate multiple

784 variable constraints and time delays into control scheme design, and manage inherent process  
785 variability by accounting for process disturbances. By incorporating model predictions, MPC  
786 can also forecast, and mitigate for, potential issues [101]. However, this means that the ability  
787 of MPC to control a process successfully depends strongly on the accuracy of the process  
788 model used. Despite this, MPC is a well-established and proven technique, with applications  
789 in the oil and gas industry dating back to the 1980s [102]. Note also that MPC can be used in  
790 conjunction with standard PID controllers, where the MPC controller updates PID set-points.

791 Seborg et al. [101] provide a comprehensive overview of MPC. A summary of the main steps  
792 outlined is as follows. Firstly, a process model is used to make current and future predictions  
793 of key output variables over a short timeframe. MPC uses a dynamic process model to make  
794 predictions, usually a linear empirical model or a linearised version of a complex non-linear  
795 model. Secondly, the predictions are used to compute optimal process set-points over the  
796 timeframe using a steady-state version of the dynamic model. This steady-state optimisation  
797 generally uses a basic objective function, such as maximising production rate or minimising a  
798 cost function. Thirdly, the calculated set-points are fed into subsequent control calculations to  
799 determine a sequence of optimal control actions using the dynamic process model. The control  
800 actions calculated aim to drive the predicted outputs to the calculated set-points in an  
801 optimised manner, by satisfying a second specified objective function. Both the steady-state  
802 and dynamic optimisations can incorporate variable constraints, such as upper and lower  
803 boundaries for input and output variables. Despite a sequence of control actions being  
804 calculated, only the first action is enforced. After applying the immediate control action, the  
805 timeframe is shifted along a given time step, and the optimisations are repeated. The window  
806 of time over which the predictions are made and the control variables are optimised is referred  
807 to as the prediction horizon.

808 It is evident from the MPC procedure detailed above that a critical component of a successful  
809 MPC application are the optimisation steps. As optimisation is conducted twice at every time  
810 step, MPC can be computationally expensive. Therefore, to ensure the optimisation procedure  
811 can be completed rapidly, linear process models are typically employed to facilitate the use of  
812 linear optimisation algorithms [51]. As detailed in section 3.2, chromatography systems can  
813 be predicted accurately by complex non-linear mechanistic models. Optimisation using non-  
814 linear mechanistic models is time consuming, and would result in sub-optimal frequency of  
815 control actions. Therefore, in MPC development for chromatography systems, the mechanistic  
816 process model is linearised via regression-based techniques such as system identification  
817 [103]. This facilitates the use of linear optimisation algorithms, which greatly reduces the  
818 computational burden relative to the non-linear alternatives. It should be noted however, that

819 as computing power increases and non-linear optimisation strategies improve, there is  
820 potential to use MPC for near real-time non-linear control [51].

821 Examples of MPC for chromatography processes in academia date back to the turn of the  
822 century, with the focus mainly on continuous systems and chemical products [104,105].  
823 Grossmann et al. [106] provided an in silico example of MPC to a continuous mAb purification  
824 process. The mechanistic model, composed of lumped kinetic transport and competitive  
825 Langmuir adsorption models, was linearised around a steady-state value. The reduced order  
826 model decreased the number of states from 1200 to 22, facilitating the application of a Kalman  
827 filter and computationally efficient optimisation. Optimisation and control actions were  
828 performed at the beginning of each cycle.

829 Further research has culminated in the development of the Parametric Optimisation and  
830 Control (PAROC) framework by teams at Texas A&M University and Imperial College London  
831 [107]. The PAROC framework aims to provide a standardised platform for modelling-  
832 orientated process design, optimisation and control, with a focus on deriving multiparametric  
833 MPC systems. When applied to chromatography systems, the proposed scheme consists of  
834 four main steps. Firstly, a mechanistic chromatography model is developed and validated.  
835 Secondly, the model is linearised via system identification or alternative model reduction  
836 techniques. Thirdly, a multiparametric MPC system is formulated using the linearised process  
837 model. MPC design and tuning parameters, such as the length of the prediction horizon and  
838 the sampling period, are specified. Furthermore, a map of objective function solutions, and so  
839 optimal control actions, is produced accounting for input, output and disturbance constraints.  
840 Finally, the closed-loop control system is validated in-silico on the original mechanistic model.

841 The PAROC framework has been demonstrated on continuous systems in several subsequent  
842 publications in silico [103,108–111]. In each case, multiparametric MPC is employed to obtain  
843 cyclic steady state by monitoring the integral of product and impurity concentrations (the output  
844 variables), and using “steady state shift” to carefully control the elution phase. As expected for  
845 bind/elute chromatography, the elution buffer salt concentration is identified as the significant  
846 input variable, with feed composition incorporated as an uncontrolled disturbance. Whilst feed  
847 flowrate is identified to have no significant impact on the eluted quantities, and so is excluded  
848 from the input variable set, it does impact the elution time [110]. Therefore, the control strategy  
849 was tested over a range of feed flowrates.

850 The MPC controllers demonstrated have several unique benefits. Consistent operation is  
851 obtained, whether that be through the implementation of cycle-to-cycle control actions [106]  
852 or through continuous monitoring and control action implementation [109]. The continuous  
853 chromatography process can be driven to cyclic steady state, whilst accounting for

854 disturbances in feed composition. Furthermore, the model-based controller is able to  
855 outperform non-model orientated alternatives, such as PID control (see section 3.3), owing to  
856 the enhanced understanding imbedded in the linearised process model [109]. However,  
857 several publications highlight a focal issue with model-based control for protein purification.  
858 The controllers are highly reliant on real-time measurements of protein concentrations in the  
859 feed and/or column outlet [106,108]. As described in section 2.2, there are significant  
860 drawbacks with established UV spectroscopy and HPLC-based monitoring systems.  
861 Therefore, the development of novel PATs to provide feedback to the control scheme is  
862 critical. A PAT that can accurately and rapidly monitor co-eluting components may expedite  
863 the transition from MPC as an in silico control technique, to a proven control strategy for protein  
864 purification at industrial scale.

#### 865 **4. The future of industrial chromatography control systems**

866 Based on the previous discussion, there is a need for advanced chromatography control  
867 strategies. The application of these state-of-the-art PATs and control strategies to future  
868 industrial chromatography processes must be done on a case by case basis. First, the  
869 implementation of PAT such as Raman or NIR for process monitoring comes with additional  
870 costs. Second, the implementation of new PATs and the development of control strategies  
871 requires experts trained in the use of the PATs and in the development of statistical and/or  
872 mechanistic models for control. Finally, there must be enough confidence in the statistical  
873 and/or mechanistic models of these tools for industry and regulators to approve them over  
874 proven off-line quantification methods.

875 A schematic of a potential advanced chromatography control strategy is shown in Figure 5.  
876 The design uses several PATs to monitor key process parameters as well as information from  
877 upstream PAT. Although the figure shows a continuous chromatography set up, the design is  
878 also applicable to a batch system. While batch remains commonplace, continuous offers the  
879 potential for better process productivity and efficiency as discussed in section 2.2.  
880 Furthermore, continuous chromatography works efficiently with perfusion bioreactors, which  
881 operate for longer periods of times than batch bioreactors, constantly producing product with  
882 lower product composition variations than batch. In a batch chromatography system, the  
883 design would remain the same save for removal of the column switching loop.

884 Figure 5 includes a single control unit which can be mechanistic, statistical, or a hybrid of these  
885 two, the nature of the model being dependent on the process in question. This control unit  
886 utilises a process model that can be mechanistic, statistical, or a hybrid of these two, the  
887 nature of the model being dependent on the process in question. The main control unit makes  
888 decisions for each control sub-loop based on the data generated from the PAT in all the sub-

889 loops. In this way, the response of each control subsystem is dependent on the state of the  
890 entire process. To streamline the discussion of Figure 5, the figure discussion is broken down  
891 by the individual control loops presented and their importance to the control of the overall  
892 process. These control loops are the column switching, production fractionation, column  
893 fouling, and external IC loops.

894 **Column Switching Control Loop:** As demonstrated in the red control loop, efficient and  
895 timely column switching in continuous chromatography improves process efficiency and  
896 reduces column to column variation. Traditionally, column switching in continuous  
897 chromatography systems is performed by timed switches determined through previous  
898 experimental analysis. Due to the limitations of timed column switching discussed in section  
899 2.2, column switching based on column breakthrough determined by utilising spectroscopy-  
900 based PAT offers a beneficial alternative, as demonstrated in literature (Table 3). The  
901 implementation of a column switching control loop meets regulator desires for more consistent  
902 processes and can be easily be achieved with existing product fractionation PAT (Figure 5).

903 **Fractionation Control Loop:** Highlighted in blue within the figure, fractionation control is the  
904 key to obtaining the desired product yield and purity. While traditional single-wavelength UV  
905 methods have often failed to differentiate product and product related impurities for complex  
906 separations, recent studies have overcome these challenges through advanced spectroscopy  
907 techniques and models, yielding more robust separations (Table 3). The proposed  
908 fractionation control loop makes use of a PAT at the inlet and outlet of the column system  
909 (Figure 5). The inlet PAT will be utilised to monitor the composition of the incoming feed. This  
910 information is fed to the overall empirical/mechanistic model which predicts the elution time of  
911 the product and dictates fractionation. The PAT at the outlet monitors the composition of the  
912 outlet stream, which is once again fed to the process model. As such, the PAT at the outlet  
913 composition determined by the PAT differs significantly from that predicted by the model, the  
914 outlet data can be used dictate fractionation. In this way, the ability of the feedforward model-  
915 based controller to direct fractionation with a negligible time-delay is exploited, while the  
916 validity of model predictions is monitored via feedback data from the PAT.

917 The PAT providing data to the fractionation loop will likely be spectroscopy based. However,  
918 spectroscopy techniques work well in tandem with at-line or automated on-line HPLC/UPLC.  
919 Due to its faster measurement time but lower accuracy, the spectroscopy PAT provides the  
920 primary source of feedback data to the controller. The HPLC/UPLC measurements, which  
921 take longer to produce but are more reliable, are then used to adjust the control decisions  
922 made from the spectroscopy measurements or mechanistic model. Combined control  
923 strategies utilising both off-line and on-line measurement control strategies have previously

924 been implemented in the biopharmaceutical industry, such as on fermentation control [112].  
925 For this reason, a controller utilising process data from an in-line spectroscopy PAT and an  
926 at-line or automated on-line HPLC/UPLC should be feasible. For systems with significant  
927 levels of protein aggregation, the implementation of MALS in-line or by autosampler would be  
928 beneficial in reducing and controlling the aggregate levels during the separation [75,76].  
929 Furthermore, the addition of an autosampler adds the additional benefits of previously at-line  
930 analysis, such as ELISA, MS, and/or any other complex analysis techniques [22,24]. Though  
931 the inlet and outlet PAT provide the critical data to the controller unit necessary for fractionation  
932 control, PAT are also utilised to monitor the fouling of the column.

933 **Fouling Control Loop:** Shown in green within Figure 5, the fouling control loop monitors  
934 column fouling and initiates CIP when needed. The build-up of column fouling over the course  
935 of process operation leads to lower binding capacity and therefore decreased operational  
936 efficiency. Although this is the case, most current methodologies call for CIP between a set  
937 number of column operations recommended by the manufacturer or experimentally pre-  
938 determined [113]. This may lead to CIP occurring too early or too late, leading to decreased  
939 operational efficiency or faster column degradation. Due to the substantial cost of the  
940 chromatography resin, especially protein A resin, there is a desire to maximise column  
941 lifespan. Therefore, the implementation of a fouling control loop can be used to reduce process  
942 expenses by increasing column lifespan (Figure 5). Fouling of the column can be monitored  
943 using fluorescence spectroscopy or ATR-FTIR (Table 3). If a mechanistic model is utilised to  
944 control the system, the binding capacity coefficient within the model can be adjusted based  
945 on the fouling data obtained from the PAT. Furthermore, the PAT used to monitor fouling can  
946 also be used to test the efficacy of CIP buffers, making it a versatile tool to have. The chosen  
947 PAT will monitor the column and send data to the control unit. When the fouling reaches critical  
948 levels, the controller directs the system to implement CIP. The automation of CIP helps  
949 maximises the columns lifespan and reduce labour requirements during operation.

950 **Buffer Formulation Control Loop:** Finally, highlighted within Figure 5 in purple as an external  
951 data link, the buffer formulation control loop automates buffer formulation, allowing for rapid  
952 adjustments to adapt to variations in the process. As discussed in section 2.1, automated  
953 buffer formulation using feedback control can provide a multitude of potential benefits to a  
954 biologic production facility. Benefits include a large reduction in plant footprint and CAPEX  
955 thanks to the associated reduction in buffer storage requirements, more consistent and robust  
956 buffer formulation, and a substantial reduction in labour and time requirements for buffer  
957 production [33]. Therefore, an in-line conditioning (ILC) unit has been included in Figure 5.  
958 Close control of the buffer conditions as it is produced within the ILC unit would ensure the  
959 equilibration, washing and elution stages proceed as desired. Data regarding buffer pH,

960 conductivity and salt content can also be passed to the overall process control unit, potentially  
961 informing the mechanistic or empirical model simulations used to dictate product fractionation.  
962 The process robustness and productivity improvements associated with in-line buffer  
963 formulation techniques are expected to outweigh the increased control system costs and  
964 complexity [29]. As regulatory and industry familiarity with automated buffer formulation  
965 improves, it is expected that such systems will find more regular application for industrial scale  
966 protein production as companies strive to eliminate the buffer bottleneck.

967 It should be noted that advanced chromatography control strategies should only be employed  
968 when the cost savings for the process outweigh the increased control complexity and  
969 development expenses [36]. When this is not the case, simpler or more traditional control  
970 strategies should be implemented. In a simple separation, where the product-related  
971 impurities are limited and/or the resolution between the product and impurities is good, a  
972 simple control system can be utilised. In such a case, model predictability of the system is  
973 likely to be good. As a result, a well-developed and validated mechanistic model may be all  
974 that is required to control the process. If a spectroscopy PAT is utilised for monitoring or  
975 control, only one or two UV wavelengths may need to be monitored rather than a spectra due  
976 to the high resolution between product and impurities.

977 For more complex separations, with significant amounts of product-related impurities and low  
978 resolutions between product and impurities, a more complex controller, such as a hybrid  
979 control strategy utilising a mechanistic model coupled with a MVDA based PAT model, will be  
980 required. In a hybrid control system, the mechanistic model makes elution time and process  
981 predictions based on the composition of the feed stream, column fouling, and other process  
982 parameters. The addition of a multi-wavelength spectroscopy system, utilising a MVDA model,  
983 is useful for two reasons. First, low concentration impurities are challenging to quantify in-line,  
984 and to predict accurately with mechanistic or empirical models. In such cases, the control  
985 system may benefit from both models working in tandem. The spectroscopy-MVDA model  
986 measures the total protein concentration while the mechanistic model predicts the product  
987 concentration. By subtracting the predicted product concentration from the total measured  
988 concentration, the protein impurity concentration can be predicted. This is then used to  
989 calculate product purity and to fractionate accordingly. Second, the MVDA model monitors for  
990 any deviations between the mechanistic model prediction and actual process operation. If  
991 significant deviations are found, then the MVDA side of the model can step in to correct the  
992 process, and maintain product consistency and operational robustness. Furthermore, this  
993 could trigger a mechanistic model recalibration, using an inverse-fit method and the  
994 deconvoluted signal from the spectroscopy system to update the model parameters.

995 **5. Conclusion**

996 This paper reviews the growing body of research related to industrial chromatography control  
997 for biotherapeutics revealing significant promise that chromatography control will attain the  
998 same degree of robustness and rapid response as seen in control systems in traditional  
999 process industries. While the implementation of PAT and process control methods do require  
1000 additional time and cost to develop, they have the potential to fulfil the additional control  
1001 requirements. Future work will include an in-depth cost analysis to help determine the balance  
1002 between the upfront costs for developing and implementing advanced control strategies, and  
1003 the expected savings during process development and product manufacture as a result of  
1004 enhanced process robustness and productivity. Several advanced industrial chromatography  
1005 control strategies outlined in this review have demonstrated increased robustness and  
1006 improved control of product quality attributes, with the potential to become an integral part of  
1007 biopharmaceutical process development and commercial manufacturing in the future.

1008 **6. Acknowledgements**

1009 We would like to thank the UCL Decisional Tools research group, the UCL Recovery of  
1010 Biological Products research group, and CODOBIO for their feedback on our work.  
1011 Specifically, we would like to thank Beatrice Melinek for sharing useful information and  
1012 documents with us, and Catarina Neves for her comments regarding cost analysis.

1013 **Funding**

1014 This research is associated with the joint UCL-AstraZeneca Centre of Excellence for predictive  
1015 multivariate decision support tools in the bioprocessing sector and financial support for A.A.  
1016 and K.H is gratefully acknowledged. Furthermore, support from BBSRC for K.H. and  
1017 CODOBIO for A.A. is also greatly appreciated. This project has received funding from the  
1018 European Union's Horizon 2020 research and innovation programme under the Marie  
1019 Skłodowska-Curie grant agreement No 812909 CODOBIO, within the Marie Skłodowska-  
1020 Curie European Training Networks framework.

1021 **CRedit authorship contribution statement**

1022 **Alexander Armstrong:** Conceptualization, Investigation, Writing - original draft, Writing -  
1023 review & editing. **Kieran Horry:** Conceptualization, Investigation, Writing - original draft,  
1024 Writing - review & editing. **Tingting Cui:** Supervision, Writing - review & editing. **Martyn**  
1025 **Hulley:** Supervision, Writing - review & editing. **Richard Turner:** Supervision. **Suzanne S.**  
1026 **Farid:** Supervision, Writing - review & editing. **Stephen Goldrick:** Supervision, Writing -  
1027 review & editing. **Daniel G. Bracewell:** Project administration, Supervision, Writing - review &  
1028 editing.

1029 **7. References**

- 1030 [1] Z.E. Sauna, H.A.D. Lagassé, A. Alexaki, V.L. Simhadri, N.H. Katagiri, W. Jankowski,  
1031 C. Kimchi-Sarfaty, Recent advances in (therapeutic protein) drug development,  
1032 *F1000Research*. 6 (2017). <https://doi.org/10.12688/f1000research.9970.1>.
- 1033 [2] G. Walsh, Biopharmaceutical benchmarks 2018, *Nat. Biotechnol.* 36 (2018) 1136–  
1034 1145. <https://doi.org/10.1038/nbt.4305>.
- 1035 [3] M. Kessel, The problems with today's pharmaceutical business—an outsider's view,  
1036 *Nat. Publ. Gr.* 29 (2011) 27–33. <https://doi.org/10.1038/nbt0111-27>.
- 1037 [4] J.W. Scannell, A. Blanckley, H. Boldon, B. Warrington, Diagnosing the decline in  
1038 pharmaceutical R&D efficiency, *Nat. Rev. Drug Discov.* 11 (2012) 191–200.  
1039 <https://doi.org/10.1038/nrd3681>.
- 1040 [5] O.J. Wouters, M. McKee, J. Luyten, Estimated Research and Development Investment  
1041 Needed to Bring a New Medicine to Market, 2009-2018, *JAMA - J. Am. Med. Assoc.*  
1042 323 (2020) 844–853. <https://doi.org/10.1001/jama.2020.1166>.
- 1043 [6] A.L. Grilo, A. Mantalaris, The Increasingly Human and Profitable Monoclonal Antibody  
1044 Market, *Trends Biotechnol.* 37 (2019) 9–16.  
1045 <https://doi.org/10.1016/j.tibtech.2018.05.014>.
- 1046 [7] P. Gagnon, Technology trends in antibody purification, *J. Chromatogr. A.* 1221 (2012)  
1047 57–70. <https://doi.org/10.1016/j.chroma.2011.10.034>.
- 1048 [8] M. Bisschops, M. Brower, The impact of continuous multicolumn chromatography on  
1049 biomanufacturing efficiency, *Pharm. Bioprocess.* 1 (2013) 361–372.  
1050 <https://doi.org/10.4155/pbp.13.46>.
- 1051 [9] C. Tsouris, J. V. Porcelli, Process Intensification - Has Its Time Finally Come?, *Chem.*  
1052 *Eng. Prog.* 99 (2003) 50–55.
- 1053 [10] C. Chen, H.E. Wong, C.T. Goudar, Upstream process intensification and continuous  
1054 manufacturing, *Curr. Opin. Chem. Eng.* 22 (2018) 191–198.  
1055 <https://doi.org/10.1016/j.coche.2018.10.006>.
- 1056 [11] J. Strube, R. Ditz, M. Kornecki, M. Huter, A. Schmidt, H. Thiess, S. Zobel-Roos, Process  
1057 intensification in biologics manufacturing, *Chem. Eng. Process. - Process Intensif.* 133  
1058 (2018) 278–293. <https://doi.org/10.1016/j.cep.2018.09.022>.
- 1059 [12] R. Peña, Z.K. Nagy, Process Intensification through Continuous Spherical  
1060 Crystallization Using a Two-Stage Mixed Suspension Mixed Product Removal

- 1061 (MSMPR) System, *Cryst. Growth Des.* 15 (2015) 4225–4236.  
1062 <https://doi.org/10.1021/acs.cgd.5b00479>.
- 1063 [13] D. Yilmaz, H. Mehdizadeh, D. Navarro, A. Shehzad, M. O'Connor, P. McCormick,  
1064 Application of Raman spectroscopy in monoclonal antibody producing continuous  
1065 systems for downstream process intensification, *Biotechnol. Prog.* 36 (2020).  
1066 <https://doi.org/10.1002/btpr.2947>.
- 1067 [14] J.M. Juran, *Juran on quality by design: the new steps for planning quality into goods*  
1068 *and services*, Simon and Schuster, 1992.
- 1069 [15] FDA, ICH Q8(R2) Pharmaceutical Development, *Work. Qual. by Des. Pharm.* 8 (2009)  
1070 28.
- 1071 [16] L.X. Yu, G. Amidon, M.A. Khan, S.W. Hoag, J. Polli, G.K. Raju, J. Woodcock,  
1072 Understanding pharmaceutical quality by design, *AAPS J.* 16 (2014) 771–783.  
1073 <https://doi.org/10.1208/s12248-014-9598-3>.
- 1074 [17] C. Finkler, L. Krummen, Introduction to the application of QbD principles for the  
1075 development of monoclonal antibodies, *Biologicals.* (2016).  
1076 <https://doi.org/10.1016/j.biologicals.2016.07.004>.
- 1077 [18] CMC Biotech Working Group, *A-Mab: a Case Study in Bioprocess Development*  
1078 (Version 2.1), (2009).
- 1079 [19] D. Baur, J. Angelo, S. Chollangi, T. Müller-Späth, X. Xu, S. Ghose, Z.J. Li, M. Morbidelli,  
1080 Model-assisted process characterization and validation for a continuous two-column  
1081 protein A capture process, *Biotechnol. Bioeng.* 116 (2019) 87–98.  
1082 <https://doi.org/10.1002/bit.26849>.
- 1083 [20] FDA, *Pharmaceutical CGMPs for the 21st Century - A risk-based approach*, *Food Drug*  
1084 *Adm.* (2004) 32.  
1085 [http://www.fda.gov/Drugs/DevelopmentApprovalProcess/Manufacturing/Questionsand](http://www.fda.gov/Drugs/DevelopmentApprovalProcess/Manufacturing/QuestionsandAnswers/CurrentGoodManufacturingPracticescGMPforDrugs/UCM071836)  
1086 [AnswersonCurrentGoodManufacturingPracticescGMPforDrugs/UCM071836](http://www.fda.gov/Drugs/DevelopmentApprovalProcess/Manufacturing/QuestionsandAnswers/CurrentGoodManufacturingPracticescGMPforDrugs/UCM071836).
- 1087 [21] L. Rolinger, M. Rüdert, J. Hubbuch, A critical review of recent trends, and a future  
1088 perspective of optical spectroscopy as PAT in biopharmaceutical downstream  
1089 processing, *Anal. Bioanal. Chem.* 412 (2020) 2047–2064.  
1090 <https://doi.org/10.1007/s00216-020-02407-z>.
- 1091 [22] D.P. Wasalathanthri, M.S. Rehmann, Y. Song, Y. Gu, L. Mi, C. Shao, L. Chemmalil, J.  
1092 Lee, S. Ghose, M.C. Borys, J. Ding, Z.J. Li, *Technology Outlook for Real Time Quality*

- 1093 Attribute and Process Parameter Monitoring in Biopharmaceutical Development – A  
1094 Review, *Biotechnol. Bioeng.* (2020) bit.27461. <https://doi.org/10.1002/bit.27461>.
- 1095 [23] F. Feidl, S. Vogg, M. Wolf, M. Podobnik, C. Ruggeri, N. Ulmer, R. Wälchli, J. Souquet,  
1096 H. Broly, A. Butté, M. Morbidelli, Process-wide control and automation of an integrated  
1097 continuous manufacturing platform for antibodies, *Biotechnol. Bioeng.* 117 (2020)  
1098 1367–1380. <https://doi.org/10.1002/bit.27296>.
- 1099 [24] M.K. Maruthamuthu, S.R. Rudge, A.M. Ardekani, M.R. Ladisch, M.S. Verma, Process  
1100 Analytical Technologies and Data Analytics for the Manufacture of Monoclonal  
1101 Antibodies, *Trends Biotechnol.* (2020). <https://doi.org/10.1016/j.tibtech.2020.07.004>.
- 1102 [25] M. Jiang, K.A. Severson, J.C. Love, H. Madden, P. Swann, L. Zang, R.D. Braatz,  
1103 Opportunities and challenges of real-time release testing in biopharmaceutical  
1104 manufacturing, *Biotechnol. Bioeng.* 114 (2017) 2445–2456.  
1105 <https://doi.org/10.1002/bit.26383>.
- 1106 [26] EMA, Guideline on Real Time Release Testing (formerly Guideline on Parametric  
1107 Release). European Medicines Agency, Committee for Medicinal Products for Human  
1108 Use, 2012.
- 1109 [27] ICH, Guidance for Industry Q8(R2) Pharmaceutical Development, 2009.
- 1110 [28] FDA, Guidance for Industry PAT - A Framework for Innovative Pharmaceutical  
1111 Development, manufacturing, and Quality Assurance, 2004.
- 1112 [29] E.N. Carredano, R. Nordberg, S. Westin, K. Busson, T.M. Karlsson, T.S. Blank, H.  
1113 Sandegren, G. Jagschies, Simplification of Buffer Formulation and Improvement of  
1114 Buffer Control with In-Line Conditioning (IC), in: *Biopharm. Process. Dev. Des.*  
1115 *Implement. Manuf. Process.*, 2018. [https://doi.org/10.1016/B978-0-08-100623-](https://doi.org/10.1016/B978-0-08-100623-8.00027-X)  
1116 [8.00027-X](https://doi.org/10.1016/B978-0-08-100623-8.00027-X).
- 1117 [30] H. Schmidt-Traub, M. Schulte, A. Seidel-Morgenstern, *Preparative Chromatography:*  
1118 *Second Edition*, Wiley-VCH, Weinheim, Germany, 2013.  
1119 <https://doi.org/10.1002/9783527649280>.
- 1120 [31] T. Matthews, B. Bean, P. Mulherkar, B. Wolk, An Integrated Approach to Buffer Dilution  
1121 and Storage, *Pharma Manuf.* (2009).
- 1122 [32] M. Li, V. Kamat, H. Yabe, T. Miyabayashi, S. Jariwala, Process Analytical Technology-  
1123 Based In-Line Buffer Dilution: In Downstream Bioprocessing, *Pharm. Technol.* (2010).
- 1124 [33] D. Fabbrini, C. Simonini, J. Lundkvist, E. Carredano, D. Otero, Addressing the

- 1125 Challenge of Complex Buffer Management: An In-Line Conditioning Collaboration,  
1126 Bioprocess Int. (2017).
- 1127 [34] M. Rüdts, T. Briskot, J. Hubbuch, Advances in downstream processing of biologics –  
1128 Spectroscopy: An emerging process analytical technology, *J. Chromatogr. A.* 1490  
1129 (2017) 2–9. <https://doi.org/10.1016/j.chroma.2016.11.010>.
- 1130 [35] N. Borg, Y. Brodsky, J. Moscariello, S. Vunnum, G. Vedantham, K. Westerberg, B.  
1131 Nilsson, Modeling and robust pooling design of a preparative cation-exchange  
1132 chromatography step for purification of monoclonal antibody monomer from  
1133 aggregates, *J. Chromatogr. A.* 1359 (2014) 170–181.  
1134 <https://doi.org/10.1016/j.chroma.2014.07.041>.
- 1135 [36] O. Kaltenbrunner, Y. Lu, A. Sharma, K. Lawson, T. Tressel, Risk-benefit evaluation of  
1136 on-line high-performance liquid chromatography analysis for pooling decisions in large-  
1137 scale chromatography, *J. Chromatogr. A.* 1241 (2012) 37–45.  
1138 <https://doi.org/10.1016/j.chroma.2012.04.003>.
- 1139 [37] A.S. Rathore, R. Wood, A. Sharma, S. Dermawan, Case study and application of  
1140 process analytical technology (PAT) towards bioprocessing: II. Use of ultra-  
1141 performance liquid chromatography (UPLC) for making real-time pooling decisions for  
1142 process chromatography, *Biotechnol. Bioeng.* 101 (2008) 1366–1374.  
1143 <https://doi.org/10.1002/bit.21982>.
- 1144 [38] A.S. Rathore, M.; Yu, S.; Yeboah, A.; Sharma, Case study and application of process  
1145 analytical technology (PAT) towards bioprocessing: Use of on-line high-performance  
1146 liquid chromatography (HPLC) for making real-time pooling decisions for process  
1147 chromatography, *Biotechnol. Bioeng.* 100 (2008) 306–316.  
1148 <https://doi.org/10.1002/bit.21759>.
- 1149 [39] D.B. Broughton, C.G. Gerhold, Continuous sorption process employing fixed bed of  
1150 sorbent and moving inlets and outlets, US2985589A, 1961.
- 1151 [40] V. Warikoo, R. Godawat, K. Brower, S. Jain, D. Cummings, E. Simons, T. Johnson, J.  
1152 Walther, M. Yu, B. Wright, J. Mclarty, K.P. Karey, C. Hwang, W. Zhou, F. Riske, K.  
1153 Konstantinov, Integrated continuous production of recombinant therapeutic proteins,  
1154 *Biotechnol. Bioeng.* 109 (2012) 3018–3029. <https://doi.org/10.1002/bit.24584>.
- 1155 [41] V. Girard, N.J. Hilbold, C.K.S. Ng, L. Pegon, W. Chahim, F. Rousset, V. Monchois,  
1156 Large-scale monoclonal antibody purification by continuous chromatography, from  
1157 process design to scale-up, *J. Biotechnol.* 213 (2015) 65–73.

- 1158 <https://doi.org/10.1016/j.jbiotec.2015.04.026>.
- 1159 [42] R. Godawat, K. Brower, S. Jain, K. Konstantinov, F. Riske, V. Warikoo, Periodic  
1160 counter-current chromatography - design and operational considerations for integrated  
1161 and continuous purification of proteins, *Biotechnol. J.* 7 (2012) 1496–1508.  
1162 <https://doi.org/10.1002/biot.201200068>.
- 1163 [43] J. Pollock, J. Coffman, S. V. Ho, S.S. Farid, Integrated continuous bioprocessing:  
1164 Economic, operational, and environmental feasibility for clinical and commercial  
1165 antibody manufacture, *Biotechnol. Prog.* 33 (2017) 854–866.  
1166 <https://doi.org/10.1002/btpr.2492>.
- 1167 [44] E. Mahajan, A. George, B. Wolk, Improving affinity chromatography resin efficiency  
1168 using semi-continuous chromatography, *J. Chromatogr. A.* 1227 (2012) 154–162.  
1169 <https://doi.org/10.1016/j.chroma.2011.12.106>.
- 1170 [45] J. Pollock, G. Bolton, J. Coffman, S. V. Ho, D.G. Bracewell, S.S. Farid, Optimising the  
1171 design and operation of semi-continuous affinity chromatography for clinical and  
1172 commercial manufacture, *J. Chromatogr. A.* 1284 (2013) 17–27.  
1173 <https://doi.org/10.1016/j.chroma.2013.01.082>.
- 1174 [46] A.S. Rathore, S. Mittal, S. Lute, K. Brorson, Chemometrics applications in  
1175 biotechnology processes: Predicting column integrity and impurity clearance during  
1176 reuse of chromatography resin, *Biotechnol. Prog.* 28 (2012) 1308–1314.  
1177 <https://doi.org/10.1002/btpr.1610>.
- 1178 [47] C.L. Gargalo, I. Udugama, K. Pontius, P.C. Lopez, R.F. Nielsen, A. Hasanzadeh, S.S.  
1179 Mansouri, C. Bayer, H. Junicke, K. V. Gernaey, Towards smart biomanufacturing: a  
1180 perspective on recent developments in industrial measurement and monitoring  
1181 technologies for bio-based production processes, *J. Ind. Microbiol. Biotechnol.* (2020)  
1182 1–18. <https://doi.org/10.1007/s10295-020-02308-1>.
- 1183 [48] R. Luttmann, D.G. Bracewell, G. Cornelissen, K. V. Gernaey, J. Glassey, V.C. Hass, C.  
1184 Kaiser, C. Preusse, G. Striedner, C.F. Mandenius, Soft sensors in bioprocessing: A  
1185 status report and recommendations, *Biotechnol. J.* 7 (2012) 1040–1048.  
1186 <https://doi.org/10.1002/biot.201100506>.
- 1187 [49] C.F. Mandenius, R. Gustavsson, Mini-review: Soft sensors as means for PAT in the  
1188 manufacture of bio-therapeutics, *J. Chem. Technol. Biotechnol.* 90 (2015) 215–227.  
1189 <https://doi.org/10.1002/jctb.4477>.
- 1190 [50] J.M. Vargas, S. Nielsen, V. Cárdenas, A. Gonzalez, E.Y. Aymat, E. Almodovar, G.

- 1191 Classe, Y. Colón, E. Sanchez, R.J. Romañach, Process analytical technology in  
1192 continuous manufacturing of a commercial pharmaceutical product, *Int. J. Pharm.* 538  
1193 (2018) 167–178. <https://doi.org/10.1016/j.ijpharm.2018.01.003>.
- 1194 [51] S.L. Brunton, J.N. Kutz, *Data-Driven Science and Engineering*, 2019.  
1195 <https://doi.org/10.1017/9781108380690>.
- 1196 [52] B.H. Mevik, R. Wehrens, The pls package: Principal component and partial least  
1197 squares regression in R, *J. Stat. Softw.* (2007). <https://doi.org/10.18637/jss.v018.i02>.
- 1198 [53] T. Mehmood, K.H. Liland, L. Snipen, S. Sæbø, A review of variable selection methods  
1199 in Partial Least Squares Regression, *Chemom. Intell. Lab. Syst.* (2012).  
1200 <https://doi.org/10.1016/j.chemolab.2012.07.010>.
- 1201 [54] S. Goldrick, A. Umprecht, A. Tang, R. Zakrzewski, M. Cheeks, R. Turner, A. Charles,  
1202 K. Les, M. Hulley, C. Spencer, S.S. Farid, High-Throughput Raman Spectroscopy  
1203 Combined with Innovate Data Analysis Workflow to Enhance Biopharmaceutical  
1204 Process Development, *Processes*. 8 (2020) 1179. <https://doi.org/10.3390/pr8091179>.
- 1205 [55] S. Goldrick, W. Holmes, N.J. Bond, G. Lewis, M. Kuiper, R. Turner, S.S. Farid,  
1206 Advanced multivariate data analysis to determine the root cause of trisulfide bond  
1207 formation in a novel antibody-peptide fusion, *Biotechnol. Bioeng.* 114 (2017) 2222–  
1208 2234. <https://doi.org/10.1002/bit.26339>.
- 1209 [56] N. Andersson, A. Löfgren, M. Olofsson, A. Sellberg, B. Nilsson, P. Tiainen, Design and  
1210 control of integrated chromatography column sequences, *Biotechnol. Prog.* 33 (2017)  
1211 923–930. <https://doi.org/10.1002/btpr.2434>.
- 1212 [57] R.A. Chmielowski, L. Mathiasson, H. Blom, D. Go, H. Ehring, H. Khan, H. Li, C. Cutler,  
1213 K. Lacki, N. Tugcu, D. Roush, Definition and dynamic control of a continuous  
1214 chromatography process independent of cell culture titer and impurities, *J. Chromatogr.*  
1215 *A.* 1526 (2017) 58–69. <https://doi.org/10.1016/j.chroma.2017.10.030>.
- 1216 [58] N. Brestrich, A. Sanden, A. Kraft, K. Mccann, J. Bertolini, J. Hubbuch, Advances in  
1217 inline quantification of co-eluting proteins in chromatography: Process-data-based  
1218 model calibration and application towards real-life separation issues, *Biotechnol.*  
1219 *Bioeng.* 112 (2015) 1406–1416. <https://doi.org/10.1002/bit.25546>.
- 1220 [59] S.K. Hansen, B. Jamali, J. Hubbuch, Selective high throughput protein quantification  
1221 based on UV absorption spectra, *Biotechnol. Bioeng.* 110 (2013) 448–460.  
1222 <https://doi.org/10.1002/bit.24712>.

- 1223 [60] M. Rüdts, N. Brestrich, L. Rolinger, J. Hubbuch, Real-time monitoring and control of the  
1224 load phase of a protein A capture step, *Biotechnol. Bioeng.* 114 (2017) 368–373.  
1225 <https://doi.org/10.1002/bit.26078>.
- 1226 [61] F. Steinebach, M. Angarita, D.J. Karst, T. Müller-Späth, M. Morbidelli, Model based  
1227 adaptive control of a continuous capture process for monoclonal antibodies production,  
1228 *J. Chromatogr. A.* 1444 (2016) 50–56. <https://doi.org/10.1016/j.chroma.2016.03.014>.
- 1229 [62] G. Thakur, V. Hebhi, A.S. Rathore, An NIR-based PAT approach for real-time control  
1230 of loading in Protein A chromatography in continuous manufacturing of monoclonal  
1231 antibodies, *Biotechnol. Bioeng.* 117 (2020) 673–686. <https://doi.org/10.1002/bit.27236>.
- 1232 [63] M. Boulet-audet, S.G. Kazarian, B. Byrne, In-column ATR-FTIR spectroscopy to  
1233 monitor affinity chromatography purification of monoclonal antibodies, *Nat. Publ. Gr.*  
1234 (2016) 1–13. <https://doi.org/https://doi.org/10.1038/srep30526>.
- 1235 [64] A. Edelmann, B. Lendl, Toward the optical tongue: Flow-through sensing of tannin-  
1236 protein interactions based on FTIR spectroscopy, *J. Am. Chem. Soc.* 124 (2002)  
1237 14741–14747. <https://doi.org/10.1021/ja026309v>.
- 1238 [65] M. Pathak, K. Lintern, T.F. Johnson, A.M. Nair, S. Mukherji, D.G. Bracewell, A.S.  
1239 Rathore, Analytical tools for monitoring changes in physical and chemical properties of  
1240 chromatography resin upon reuse, *Electrophoresis.* 40 (2019) 3074–3083.  
1241 <https://doi.org/10.1002/elps.201900089>.
- 1242 [66] M. Pathak, A.S. Rathore, Implementation of a fluorescence based PAT control for  
1243 fouling of protein A chromatography resin, *J. Chem. Technol. Biotechnol.* 92 (2017)  
1244 2799–2807. <https://doi.org/10.1002/jctb.5358>.
- 1245 [67] K. Buckley, A.G. Ryder, Applications of Raman Spectroscopy in Biopharmaceutical  
1246 Manufacturing: A Short Review, *Appl. Spectrosc.* 71 (2017) 1085–1116.  
1247 <https://doi.org/10.1177/0003702817703270>.
- 1248 [68] F. Feidl, S. Garbellini, S. Vogg, M. Sokolov, J. Souquet, H. Broly, A. Butté, M. Morbidelli,  
1249 A new flow cell and chemometric protocol for implementing in-line Raman spectroscopy  
1250 in chromatography, *Biotechnol. Prog.* 35 (2019) 1–10.  
1251 <https://doi.org/10.1002/btpr.2847>.
- 1252 [69] F. Feidl, S. Garbellini, M.F. Luna, S. Vogg, J. Souquet, H. Broly, M. Morbidelli, A. Butté,  
1253 Combining mechanistic modeling and raman spectroscopy for monitoring antibody  
1254 chromatographic purification, *Processes.* 7 (2019). <https://doi.org/10.3390/pr7100683>.

- 1255 [70] R.L. McCreery, *Raman Spectroscopy for Chemical Analysis*, 2001.  
1256 <https://doi.org/10.1088/0957-0233/12/5/704>.
- 1257 [71] S. Feng, Z. Zheng, Y. Xu, J. Lin, G. Chen, C. Weng, D. Lin, S. Qiu, M. Cheng, Z. Huang,  
1258 L. Wang, R. Chen, S. Xie, H. Zeng, A noninvasive cancer detection strategy based on  
1259 gold nanoparticle surface-enhanced raman spectroscopy of urinary modified  
1260 nucleosides isolated by affinity chromatography, *Biosens. Bioelectron.* 91 (2017) 616–  
1261 622. <https://doi.org/10.1016/j.bios.2017.01.006>.
- 1262 [72] C. Zhou, W. Qi, E.N. Lewis, J.F. Carpenter, Characterization of Sizes of Aggregates of  
1263 Insulin Analogs and the Conformations of the Constituent Protein Molecules: A  
1264 Concomitant Dynamic Light Scattering and Raman Spectroscopy Study, *J. Pharm. Sci.*  
1265 105 (2016) 551–558. <https://doi.org/10.1016/j.xphs.2015.10.023>.
- 1266 [73] D.R. Parachalil, B. Brankin, J. McIntyre, H.J. Byrne, Raman spectroscopic analysis of  
1267 high molecular weight proteins in solution-considerations for sample analysis and data  
1268 pre-processing, *Analyst.* 143 (2018) 5987–5998. <https://doi.org/10.1039/c8an01701h>.
- 1269 [74] J. Stetefeld, S.A. McKenna, T.R. Patel, Dynamic light scattering: a practical guide and  
1270 applications in biomedical sciences, *Biophys. Rev.* 8 (2016) 409–427.  
1271 <https://doi.org/10.1007/s12551-016-0218-6>.
- 1272 [75] E. Sahin, C.J. Roberts, Size-Exclusion Chromatography with Multi-angle Light  
1273 Scattering for Elucidating Protein Aggregation Mechanisms, in: *Methods Mol. Biol.*,  
1274 2012: pp. 403–423. [https://doi.org/10.1007/978-1-61779-921-1\\_25](https://doi.org/10.1007/978-1-61779-921-1_25).
- 1275 [76] B.A. Patel, A. Gospodarek, M. Larkin, S.A. Kenrick, M.A. Haverick, N. Tugcu, M.A.  
1276 Brower, D.D. Richardson, Multi-angle light scattering as a process analytical technology  
1277 measuring real-time molecular weight for downstream process control, *MAbs.* 10 (2018)  
1278 1–6. <https://doi.org/10.1080/19420862.2018.1505178>.
- 1279 [77] N. Brestich, M. Rüdte, D. Büchler, J. Hubbuch, Selective protein quantification for  
1280 preparative chromatography using variable pathlength UV/Vis spectroscopy and partial  
1281 least squares regression, *Chem. Eng. Sci.* 176 (2018) 157–164.  
1282 <https://doi.org/10.1016/j.ces.2017.10.030>.
- 1283 [78] M. Arrio-Dupont, Fluorescence of Aromatic Amino Acids in a Pyridoxal Phosphate  
1284 Enzyme: Aspartate Aminotransferase, *Eur. J. Biochem.* 91 (1978) 369–378.  
1285 <https://doi.org/10.1111/j.1432-1033.1978.tb12689.x>.
- 1286 [79] C.P. Moon, K.G. Fleming, *Using tryptophan fluorescence to measure the stability of*  
1287 *membrane proteins folded in liposomes*, 1st ed., Elsevier Inc., 2011.

- 1288 <https://doi.org/10.1016/B978-0-12-381268-1.00018-5>.
- 1289 [80] S.M. Raja, S.S. Rawat, A. Chattopadhyay, A.K. Lala, Localization and environment of  
1290 tryptophans in soluble and membrane- bound states of a pore-forming toxin from  
1291 *Staphylococcus aureus*, *Biophys. J.* 76 (1999) 1469–1479.  
1292 [https://doi.org/10.1016/S0006-3495\(99\)77307-8](https://doi.org/10.1016/S0006-3495(99)77307-8).
- 1293 [81] C. Rausell, L. Pardo-López, J. Sánchez, C. Muñoz-Garay, C. Morera, M. Soberón, A.  
1294 Bravo, Unfolding events in the water-soluble monomeric Cry1Ab toxin during transition  
1295 to oligomeric pre-pore and membrane-inserted pore channel, *J. Biol. Chem.* 279 (2004)  
1296 55168–55175. <https://doi.org/10.1074/jbc.M406279200>.
- 1297 [82] D.G. Sauer, M. Melcher, M. Mosor, N. Walch, M. Berkemeyer, T. Scharl-Hirsch, F.  
1298 Leisch, A. Jungbauer, A. Dürauer, Real-time monitoring and model-based prediction of  
1299 purity and quantity during a chromatographic capture of fibroblast growth factor 2,  
1300 *Biotechnol. Bioeng.* 116 (2019) 1999–2009. <https://doi.org/10.1002/bit.26984>.
- 1301 [83] N. Walch, T. Scharl, E. Felföldi, D.G. Sauer, M. Melcher, F. Leisch, A. Dürauer, A.  
1302 Jungbauer, Prediction of the Quantity and Purity of an Antibody Capture Process in  
1303 Real Time, *Biotechnol. J.* 14 (2019). <https://doi.org/10.1002/biot.201800521>.
- 1304 [84] L.K. Shekhawat, A.S. Rathore, An overview of mechanistic modeling of liquid  
1305 chromatography, *Prep. Biochem. Biotechnol.* 49 (2019) 623–638.  
1306 <https://doi.org/10.1080/10826068.2019.1615504>.
- 1307 [85] A. Osberghaus, S. Hepbildikler, S. Nath, M. Haindl, E. von Lieres, J. Hubbuch,  
1308 Optimizing a chromatographic three component separation: A comparison of  
1309 mechanistic and empiric modeling approaches, *J. Chromatogr. A.* (2012).  
1310 <https://doi.org/10.1016/j.chroma.2012.03.029>.
- 1311 [86] D. Roush, D. Asthagiri, D.K. Babi, S. Benner, C. Bilodeau, G. Carta, P. Ernst, M.  
1312 Fedesco, S. Fitzgibbon, M. Flamm, J. Griesbach, T. Grosskopf, E.B. Hansen, T. Hahn,  
1313 S. Hunt, F. Insaïdoo, A. Lenhoff, J. Lin, H. Marke, B. Marques, E. Papadakis, F.  
1314 Schlegel, A. Staby, M. Stenvang, L. Sun, P.M. Tessier, R. Todd, E. Lieres, J. Welsh, R.  
1315 Willson, G. Wang, T. Wucherpfennig, O. Zavalov, Toward in silico CMC: An industrial  
1316 collaborative approach to model-based process development , *Biotechnol. Bioeng.*  
1317 (2020). <https://doi.org/10.1002/bit.27520>.
- 1318 [87] E.J. Close, J.R. Salm, D.G. Bracewell, E. Sorensen, Modelling of industrial  
1319 biopharmaceutical multicomponent chromatography, *Chem. Eng. Res. Des.* 92 (2014)  
1320 1304–1314. <https://doi.org/10.1016/j.cherd.2013.10.022>.

- 1321 [88] E.J. Close, J.R. Salm, D.G. Bracewell, E. Sorensen, A model based approach for  
1322 identifying robust operating conditions for industrial chromatography with process  
1323 variability, *Chem. Eng. Sci.* 116 (2014) 284–295.  
1324 <https://doi.org/10.1016/j.ces.2014.03.010>.
- 1325 [89] V. Kumar, A.M. Lenhoff, Mechanistic Modeling of Preparative Column Chromatography  
1326 for Biotherapeutics, *Annu. Rev. Chem. Biomol. Eng.* 11 (2020) 235–255.  
1327 <https://doi.org/10.1146/annurev-chembioeng-102419-125430>.
- 1328 [90] V. Kumar, A.S. Rathore, Mechanistic Modeling Based PAT Implementation for Ion-  
1329 Exchange Process Chromatography of Charge Variants of Monoclonal Antibody  
1330 Products, *Biotechnol. J.* (2017). <https://doi.org/10.1002/biot.201700286>.
- 1331 [91] K. Westerberg, M. Degerman, B. Nilsson, Pooling control in variable preparative  
1332 chromatography processes, *Bioprocess Biosyst. Eng.* (2010).  
1333 <https://doi.org/10.1007/s00449-009-0335-8>.
- 1334 [92] B. Sreedhar, A. Wagler, M. Kaspereit, A. Seidel-Morgenstern, Optimal cut-times finding  
1335 strategies for collecting a target component from overloaded elution chromatograms,  
1336 *Comput. Chem. Eng.* 49 (2013) 158–169.  
1337 <https://doi.org/10.1016/j.compchemeng.2012.09.009>.
- 1338 [93] J. Gomis-Fons, H. Schwarz, L. Zhang, N. Andersson, B. Nilsson, A. Castan, A.  
1339 Solbrand, J. Stevenson, V. Chotteau, Model-based design and control of a small-scale  
1340 integrated continuous end-to-end mAb platform, *Biotechnol. Prog.* (2020).  
1341 <https://doi.org/10.1002/btpr.2995>.
- 1342 [94] S. Leweke, E. von Lieres, Chromatography Analysis and Design Toolkit (CADET),  
1343 *Comput. Chem. Eng.* (2018). <https://doi.org/10.1016/j.compchemeng.2018.02.025>.
- 1344 [95] F. Rischawy, D. Saleh, T. Hahn, S. Oelmeier, J. Spitz, S. Kluters, Good modeling  
1345 practice for industrial chromatography: Mechanistic modeling of ion exchange  
1346 chromatography of a bispecific antibody, *Comput. Chem. Eng.* 130 (2019).  
1347 <https://doi.org/10.1016/j.compchemeng.2019.106532>.
- 1348 [96] T. Briskot, F. Stückler, F. Wittkopp, C. Williams, J. Yang, S. Konrad, K. Doninger, J.  
1349 Griesbach, M. Bennecke, S. Hepbildikler, J. Hubbuch, Prediction uncertainty  
1350 assessment of chromatography models using Bayesian inference, *J. Chromatogr. A.*  
1351 1587 (2019) 101–110. <https://doi.org/10.1016/j.chroma.2018.11.076>.
- 1352 [97] H.L. Wade, PID Control, in: *Basic Adv. Regul. Control - Syst. Des. Appl.*, 3rd ed., ISA,  
1353 2017.

- 1354 [98] M. Krättli, F. Steinebach, M. Morbidelli, Online control of the twin-column countercurrent  
1355 solvent gradient process for biochromatography, *J. Chromatogr. A.* 1293 (2013) 51–59.  
1356 <https://doi.org/10.1016/j.chroma.2013.03.069>.
- 1357 [99] M. Krättli, G. Ströhlein, L. Aumann, T. Müller-Späth, M. Morbidelli, Closed loop control  
1358 of the multi-column solvent gradient purification process, *J. Chromatogr. A.* (2011).  
1359 <https://doi.org/10.1016/j.chroma.2011.09.081>.
- 1360 [100] T. Müller-Späth, L. Aumann, L. Melter, G. Ströhlein, M. Morbidelli, Chromatographic  
1361 separation of three monoclonal antibody variants using multicolumn countercurrent  
1362 solvent gradient purification (MCSGP), *Biotechnol. Bioeng.* (2008).  
1363 <https://doi.org/10.1002/bit.21843>.
- 1364 [101] D.E. Seborg, T.F. Edgar, D.A. Mellichamp, F.J. Doyle III, *Process dynamics and control*,  
1365 4th ed., 2016.
- 1366 [102] B.R. Mehta, Y.J. Reddy, *Industrial process automation systems: Design and*  
1367 *implementation*, 2014. <https://doi.org/10.1016/C2013-0-18954-4>.
- 1368 [103] M.M. Papathanasiou, B. Burnak, J. Katz, N. Shah, E.N. Pistikopoulos, Assisting  
1369 continuous biomanufacturing through advanced control in downstream purification,  
1370 *Comput. Chem. Eng.* 125 (2019) 232–248.  
1371 <https://doi.org/10.1016/j.compchemeng.2019.03.013>.
- 1372 [104] S. Natarajan, J.H. Lee, Repetitive model predictive control applied to a simulated  
1373 moving bed chromatography system, in: *Comput. Chem. Eng.*, 2000.  
1374 [https://doi.org/10.1016/S0098-1354\(00\)00493-2](https://doi.org/10.1016/S0098-1354(00)00493-2).
- 1375 [105] E. Kloppenburg, E.D. Gilles, Automatic control of the simulated moving bed process for  
1376 C8 aromatics separation using asymptotically exact input/output-linearization, *J.*  
1377 *Process Control.* (1999). [https://doi.org/10.1016/S0959-1524\(98\)00026-2](https://doi.org/10.1016/S0959-1524(98)00026-2).
- 1378 [106] C. Grossmann, G. Ströhlein, M. Morari, M. Morbidelli, Optimizing model predictive  
1379 control of the chromatographic multi-column solvent gradient purification (MCSGP)  
1380 process, *J. Process Control.* (2010). <https://doi.org/10.1016/j.jprocont.2010.02.013>.
- 1381 [107] E.N. Pistikopoulos, N.A. Diangelakis, R. Oberdieck, M.M. Papathanasiou, I. Nascu, M.  
1382 Sun, PAROC - An integrated framework and software platform for the optimisation and  
1383 advanced model-based control of process systems, *Chem. Eng. Sci.* (2015).  
1384 <https://doi.org/10.1016/j.ces.2015.02.030>.
- 1385 [108] M.M. Papathanasiou, F. Steinebach, M. Morbidelli, A. Mantalaris, E.N. Pistikopoulos,

1386 Intelligent, model-based control towards the intensification of downstream processes,  
1387 *Comput. Chem. Eng.* (2017). <https://doi.org/10.1016/j.compchemeng.2017.01.005>.

1388 [109] M.M. Papathanasiou, S. Avraamidou, R. Oberdieck, A. Mantalaris, F. Steinebach, M.  
1389 Morbidelli, T. Mueller-Spaeth, E.N. Pistikopoulos, Advanced control strategies for the  
1390 multicolumn countercurrent solvent gradient purification process, *AIChE J.* (2016).  
1391 <https://doi.org/10.1002/aic.15203>.

1392 [110] M.M. Papathanasiou, B. Burnak, J. Katz, N. Shah, E.N. Pistikopoulos, Control of a dual  
1393 mode separation process via multi-parametric Model Predictive Control, in: *IFAC-*  
1394 *PapersOnLine*, 2019. <https://doi.org/10.1016/j.ifacol.2019.06.191>.

1395 [111] M.M. Papathanasiou, B. Burnak, J. Katz, T. Müller-Späth, M. Morbidelli, N. Shah, E.N.  
1396 Pistikopoulos, Control of Small-Scale Chromatographic Systems Under Disturbances,  
1397 in: *Comput. Aided Chem. Eng.*, 2019. [https://doi.org/10.1016/B978-0-12-818597-](https://doi.org/10.1016/B978-0-12-818597-1.50043-6)  
1398 [1.50043-6](https://doi.org/10.1016/B978-0-12-818597-1.50043-6).

1399 [112] S. Goldrick, K. Lee, C. Spencer, W. Holmes, M. Kuiper, R. Turner, S.S. Farid, On-Line  
1400 Control of Glucose Concentration in High-Yielding Mammalian Cell Cultures Enabled  
1401 Through Oxygen Transfer Rate Measurements, *Biotechnol. J.* 13 (2018) 1700607.  
1402 <https://doi.org/10.1002/biot.201700607>.

1403 [113] A. Grönberg, M. Eriksson, M. Ersoy, H.J. Johansson, A tool for increasing the lifetime  
1404 of chromatography resins, *MABs.* 3 (2011) 192–202.  
1405 <https://doi.org/https://doi.org/10.4161/mabs.3.2.14874>.

1406 [114] BioPhorum Operations Group Ltd, In-Line Monitoring/Real-Time Release Testing in  
1407 Biopharmaceutical Processes-Prioritization and Cost-Benefit Analysis, (2020).

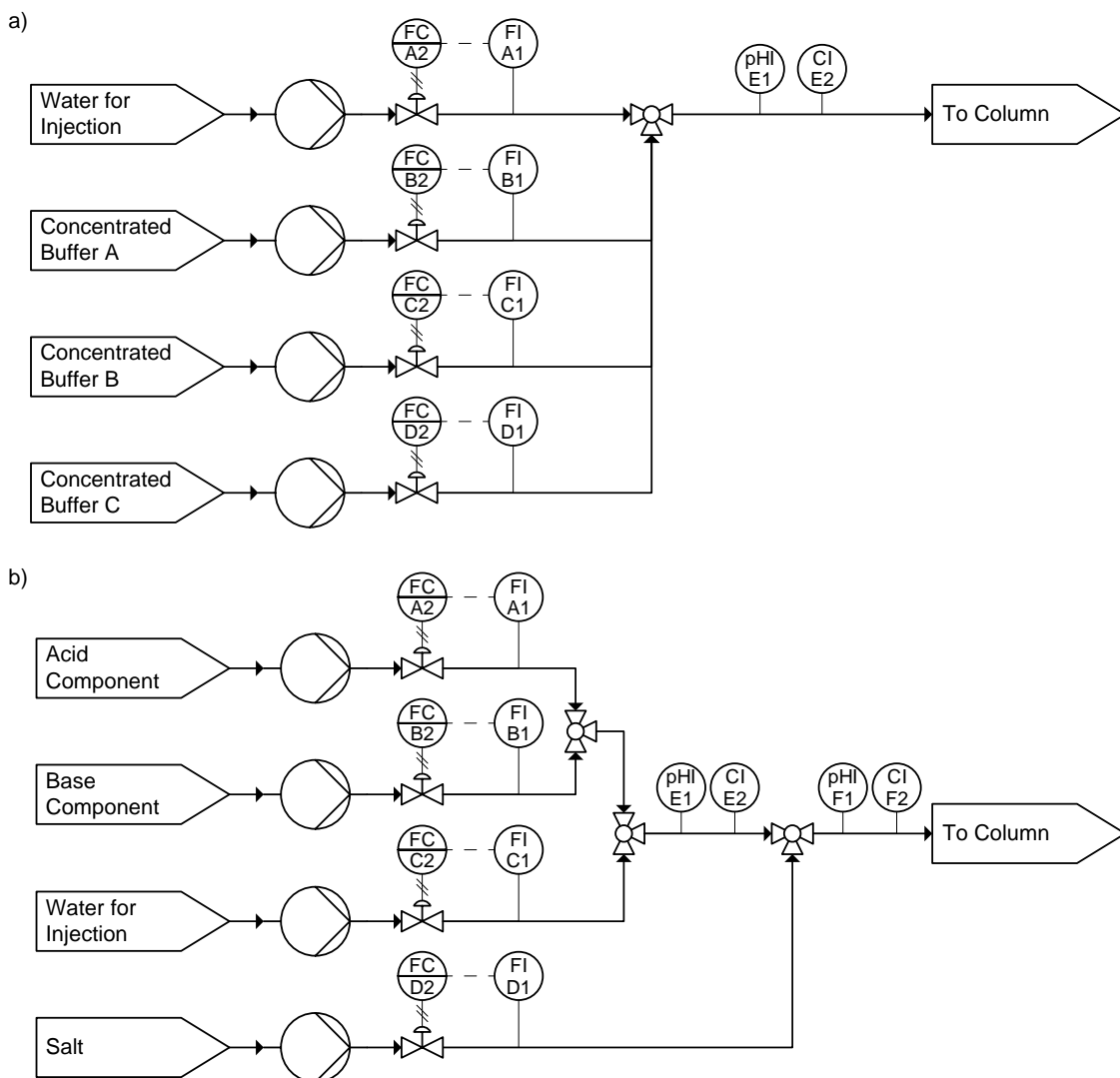
1408 [115] R.L. Fahrner, P.M. Lester, G.S. Blank, D.H. Reifsnyder, Real-time control of purified  
1409 product collection during chromatography of recombinant human insulin-like growth  
1410 factor-I using an on-line assay, *827 (1998) 37–43*.

1411 [116] A.S. Rathore, G. Kapoor, Application of process analytical technology for downstream  
1412 purification of biotherapeutics, *J. Chem. Technol. Biotechnol.* 90 (2015) 228–236.  
1413 <https://doi.org/10.1002/jctb.4447>.

1414

1415

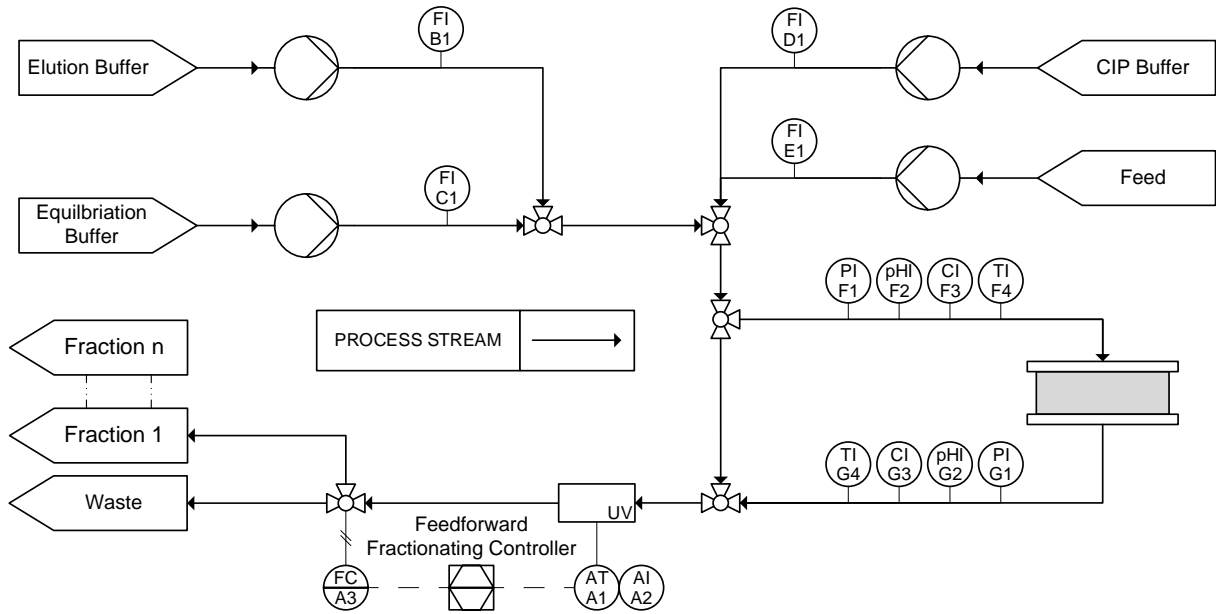
8. Figures



Key					
Name	Symbol	Name	Symbol	Name	Symbol
PUMP		PANEL MOUNTED INSTRUMENT		3-WAY VALVE	
PROCESS STREAM		LOCAL INSTRUMENT		FLOW CONTROL VALVE	
INSTRUMENT CONNECTION		PNEUMATIC SIGNAL		INTERNAL DATA LINK	
Instrument Labelling:			A – Parameter		B – Function
			<p>A - Analyser</p> <p>C - Conductivity</p> <p>F - Flow</p> <p>pH - pH</p> <p>T - Temperature</p>		<p>C - Controller</p> <p>I - Indicator</p> <p>T - Transmitter</p>
X – Control Loop ID					Y – Control Instrument ID

1417

1418 **Figure 1.** Example control schematics for an in-line buffer dilution (ILD) system (a) and an in-line  
 1419 buffer conditioning (ILC) system (b). Both schematics demonstrate feedback flow control, where the  
 1420 required input stream flowrates are determined before buffer formulation. The controllers use in-line  
 1421 flowrate measurements to ensure flowrates are at the required set-points, and that the outlet flowrate  
 1422 is maintained constant. If a deviation from the set-point is observed, the controllers adjust the flow  
 1423 control valve position to eliminate the error. Additional pH and conductivity measurements are taken  
 1424 to ensure the buffers meet the specifications prior to use.



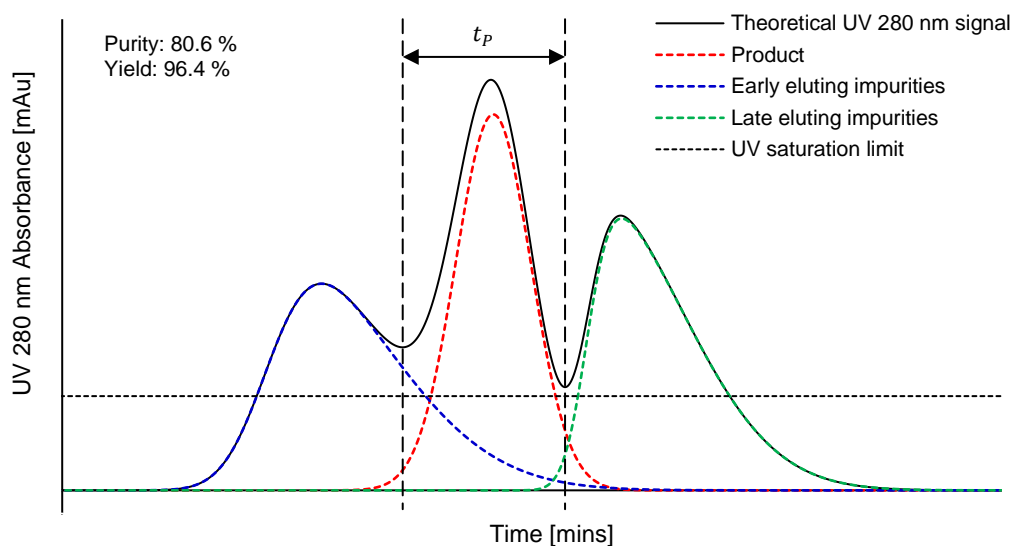
P&ID Key														
Name	Symbol	Name	Symbol	Name	Symbol									
CHROMATOGRAPHY COLUMN		PANEL MOUNTED INSTRUMENT		3-WAY VALVE										
PUMP		LOCAL INSTRUMENT		COLUMN SWITCHING VALVE										
CONTROL UNIT		UV SPECTROPHOTOMETER		INSTRUMENT CONNECTION										
PNEUMATIC SIGNAL		ELECTRICAL SIGNAL		INTERNAL DATA LINK										
Instrument Labelling:			A – Parameter		B – Function									
			<table border="0"> <tr> <td>A - Analyser</td> <td>C - Controller</td> </tr> <tr> <td>C - Conductivity</td> <td>I - Indicator</td> </tr> <tr> <td>F - Flow</td> <td>T - Transmitter</td> </tr> <tr> <td>pH - pH</td> <td></td> </tr> <tr> <td>T - Temperature</td> <td></td> </tr> </table>		A - Analyser	C - Controller	C - Conductivity	I - Indicator	F - Flow	T - Transmitter	pH - pH		T - Temperature	
A - Analyser	C - Controller													
C - Conductivity	I - Indicator													
F - Flow	T - Transmitter													
pH - pH														
T - Temperature														

1425

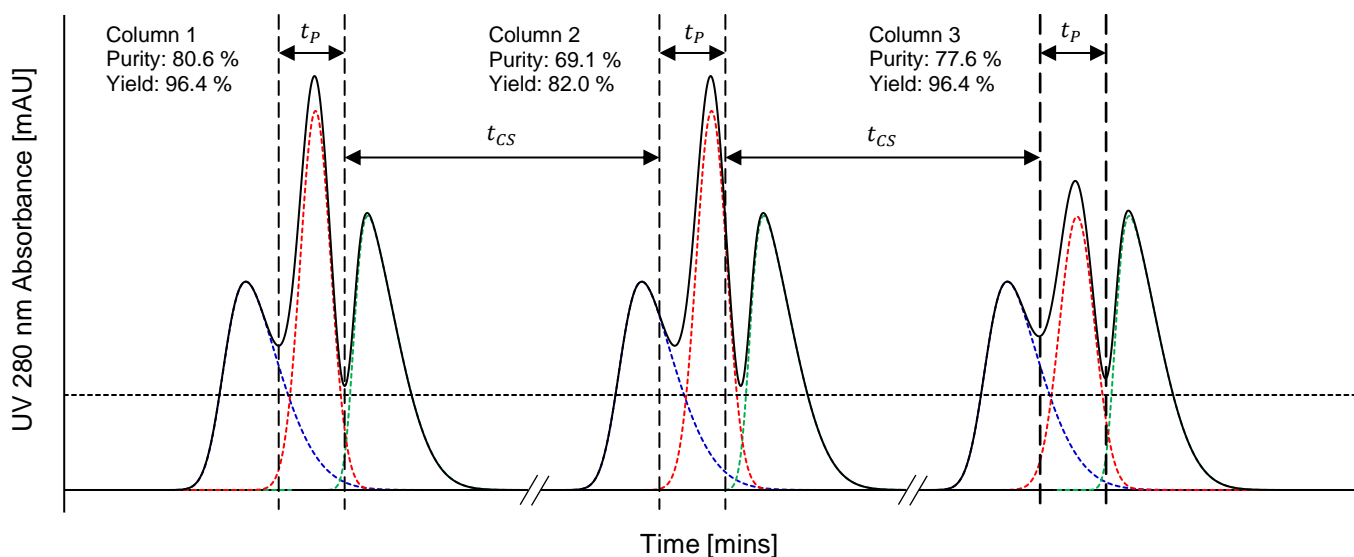
1426 **Figure 2.** Example piping and instrumentation diagram (P&ID) for a batch chromatography protein  
 1427 purification process at industrial scale. The diagram demonstrates process monitoring and control  
 1428 technologies used routinely in industry, most notably a fractionation controller. The P&ID is not  
 1429 intended to be exhaustive however, it does provide a useful overview of the relevant control and  
 1430 monitoring systems.

1431

1432 (a)

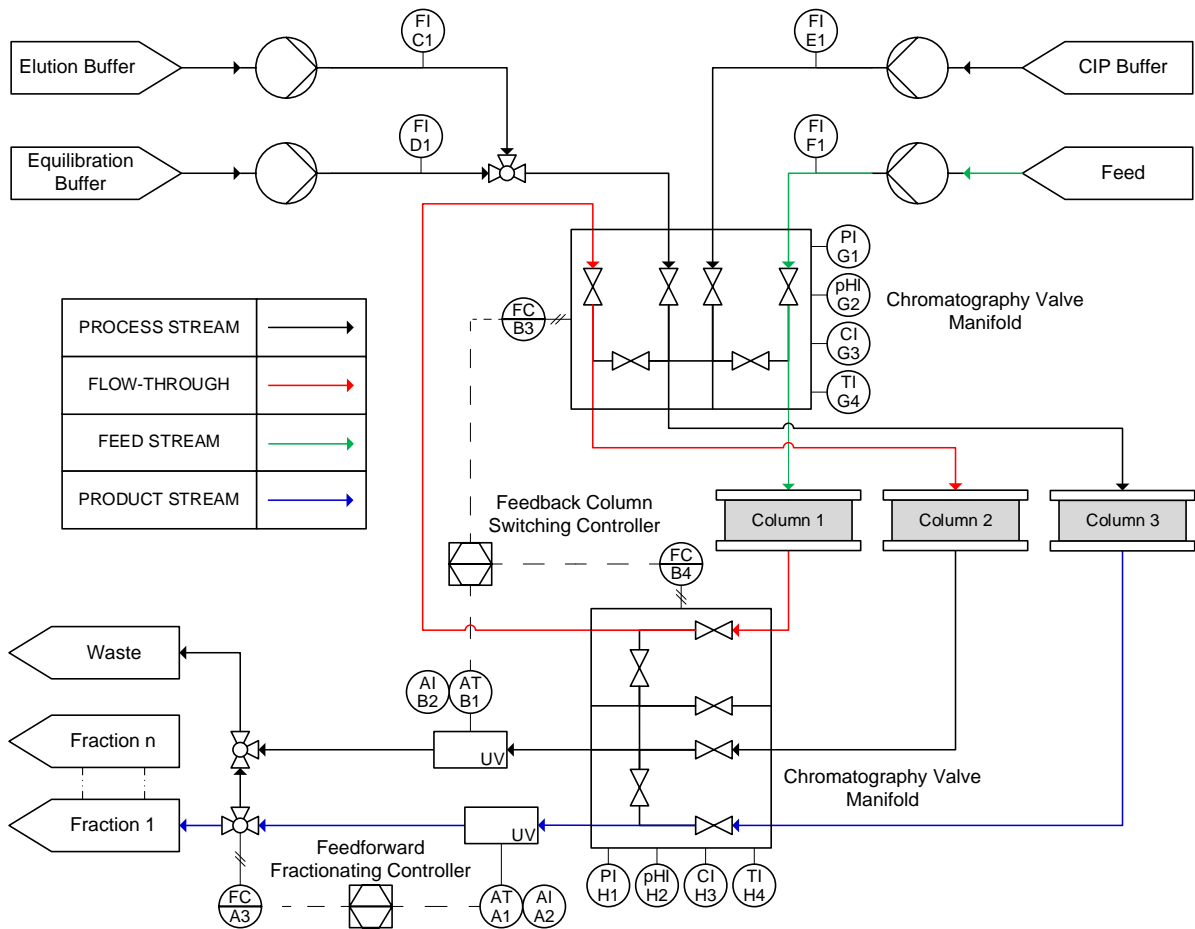


1433 (b)



1434 **Figure 3.** Example chromatograms highlighting the impact of the fractionation strategy based on UV  
 1435 280 nm monitoring at the column(s) outlet for (a) batch and (b) continuous chromatography modes  
 1436 of chromatography. In (a), product collection is instigated when the absorbance increases due to the  
 1437 presence of product in the central peak. Product collection is stopped when the UV absorbance  
 1438 increases again, due to the presence of impurities. This determines the product collection time,  $t_p$ .  
 1439 The individual absorbance of each component is plotted to demonstrate the improved insight  
 1440 obtained via spectral deconvolution. Note also that an example UV saturation limit is plotted. The  
 1441 UV 280 nm signal is unable to surpass this value if operated with a fixed pathlength. In (b), a  
 1442 traditional continuous chromatography fractionation strategy is demonstrated where the time  
 1443 between column switches,  $t_{CS}$ , and  $t_p$  are constant. Product purity and yield was calculated using  
 1444 the trapezium rule.

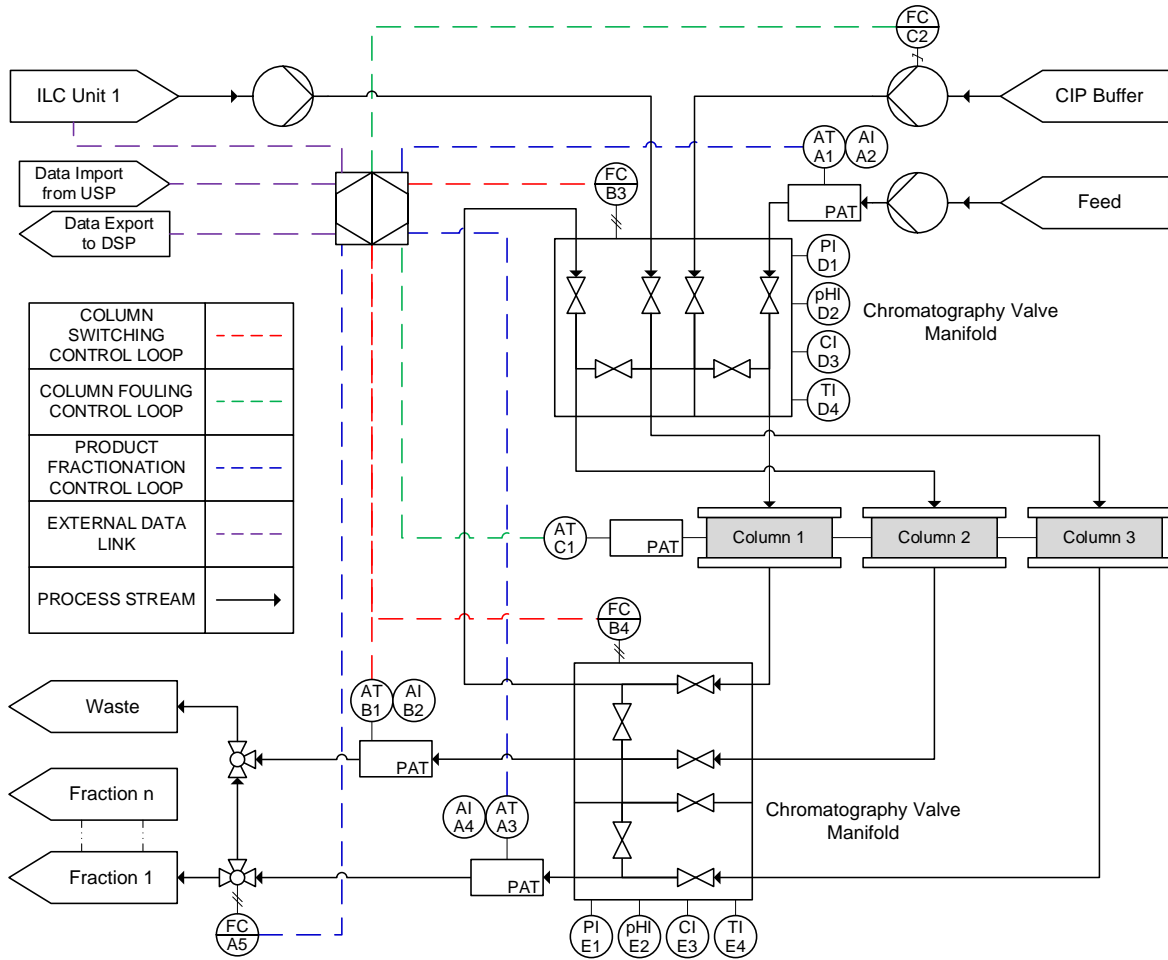
1445



P&ID Key					
Name	Symbol	Name	Symbol	Name	Symbol
CHROMATOGRAPHY COLUMN		PANEL MOUNTED INSTRUMENT		3-WAY VALVE	
PUMP		LOCAL INSTRUMENT		COLUMN SWITCHING VALVE	
CONTROL UNIT		UV SPECTROPHOTOMETER		INSTRUMENT CONNECTION	
PNEUMATIC SIGNAL		ELECTRICAL SIGNAL		INTERNAL DATA LINK	
Instrument Labelling:			A - Parameter		B - Function
A - Parameter			A - Analyser		C - Controller
X - Control Loop ID			C - Conductivity		I - Indicator
			F - Flow		T - Transmitter
			pH - pH		
			T - Temperature		

1446

1447 **Figure 4.** Example piping and instrumentation diagram (P&ID) for a three-column continuous  
 1448 chromatography protein purification process at industrial scale. The diagram demonstrates process  
 1449 monitoring and control technologies used routinely in industry, including a fractionation controller and  
 1450 a column switching controller. The P&ID highlights the flow of the feed into the system, the flow-  
 1451 through stream, and the product elution stream. The P&ID is not intended to be exhaustive however,  
 1452 it does provide a useful overview of the relevant control and monitoring systems.



P&ID Key					
Name	Symbol	Name	Symbol	Name	Symbol
CHROMATOGRAPHY COLUMN		PANEL MOUNTED INSTRUMENT		3-WAY VALVE	
PUMP		LOCAL INSTRUMENT		COLUMN SWITCHING VALVE	
ADVANCED CONTROL UNIT		PAT SPECTROPHOTOMETER		INSTRUMENT CONNECTION	
PNEUMATIC SIGNAL		ELECTRICAL SIGNAL		DATA LINK	
Instrument Labelling:			A - Parameter		B - Function
A - Parameter X - Control Loop ID					C - Controller I - Indicator T - Transmitter
			A - Analyser C - Conductivity F - Flow pH - pH T - Temperature		

1453

1454 **Figure 5.** The future outlook of chromatography control. An example piping and instrumentation  
 1455 diagrams (P&ID) for a future continuous chromatography protein purification process at industrial  
 1456 scale. The diagram demonstrates the implementation of additional Process Analytical Technologies  
 1457 (PAT) for monitoring and control of column fouling, column switching, buffer formulation, and product  
 1458 fractionation. The chromatography control unit utilizes the process data from each PAT to optimize  
 1459 the control strategies for each sub-loop. Note that flow indicators were removed from the feed  
 1460 streams to ensure that the control loops were indicated with clarity.

1461

1462

1463 **9. Tables**

1464 **Table 1.** Example product quality attributes, process parameters and performance attributes  
 1465 relevant to chromatography processes for therapeutic protein manufacturing.

Product Quality Attributes	Process Parameters	Performance Attributes
Aggregate content	Bed height	Buffer consumption
Charge profile	Elution conductivity	Process productivity
DNA content	Elution pH	Product pool concentration
Fragment content	Equilibration pH	Product pool volume
HCP content	Feed impurity content	Product yield
Leached Protein A content	Feed product concentration	Resin regeneration efficiency
Protein concentration	Load conductivity	Resin utilisation
Viral content	Load pH	
	Operating flowrate	
	Pressure	
	Product collection start time/volume	
	Product collection stop time/volume	
	Protein loading	
	Resin lifetime	
	Temperature	
	Wash conductivity	
	Wash pH	

1466 Note: Product quality attributes and process parameters may be identified as critical quality attributes (CQAs) or  
 1467 critical process parameters (CPPs) respectively via risk assessment during chromatography process development.  
 1468 However, performance attributes do not impact product quality and therefore cannot be classified as CQAs or  
 1469 CPPs but are important for process efficiency reasons [19]. The information was compiled from [18,19,25,114].

1470 **Table 2.** Summary of chromatography process control strategies in industry.

Equipment	Location	Attribute(s) Measured	Process Variable(s) Controlled	Benefits	Issues	References
In-line UV Spectrophotometer	Column outlet	Protein concentration	Product fractionation times	<ul style="list-style-type: none"> <li>• Well-established and commercially available technology</li> <li>• Cheap to purchase and operate</li> <li>• Robust operation</li> <li>• Non-invasive</li> <li>• Data obtained rapidly</li> <li>• Multiple wavelengths can be used to detect different components</li> </ul>	<ul style="list-style-type: none"> <li>• Instrument saturation likely due to limited linear range</li> <li>• Unable to differentiate between product and impurities when elution peaks overlap</li> <li>• Industrial UV detectors designed for operating robustness at the expense of sensitivity and responsiveness.</li> </ul>	[36,115,116]
On-line HPLC	Column outlet	Protein concentration	Product fractionation times	<ul style="list-style-type: none"> <li>• Well-established and commercially available technology</li> <li>• Can distinguish between product and impurities, even when they are not well resolved.</li> <li>• Can handle a wide product concentration range</li> <li>• Analysis times of under 10 minutes reported</li> <li>• Assay is well understood and reliable</li> </ul>	<ul style="list-style-type: none"> <li>• Not suitable for informing real-time control decisions</li> <li>• Potential for human error introduced if not automated</li> <li>• Additional sampling and HPLC equipment required on manufacturing floor</li> <li>• Risk of contamination increased</li> </ul>	[36,37,115,116]
In-line Buffer Dilution (ILD) System	Buffer feed to column	Flowrates of all the ILD inlet and outlet streams, and final buffer pH and conductivity	Final buffer composition, pH and conductivity	<ul style="list-style-type: none"> <li>• Substantial reduction in buffer storage requirements thereby reducing inventory, capital and cleaning costs</li> <li>• The buffer concentration can be adjusted during the process</li> <li>• Can be used to facilitate controlled gradient elution by blending buffers together</li> <li>• Feedback control improves robustness by reducing buffer variability</li> </ul>	<ul style="list-style-type: none"> <li>• Concentrated buffers require precise formulation as dilution propagates any residual formulation error</li> <li>• pH and conductivity changes must be accounted for during dilution</li> <li>• Buffer flexibility can be limited if one buffer concentrate is used to produce the final buffer</li> <li>• May require additional pumps and delivery lines to enable conductivity and pH control</li> <li>• Additional validation and maintenance costs introduced</li> </ul>	[29–32]
In-line Buffer Conditioning (ILC) System	Buffer feed to column	Flowrates of all the ILC inlet and outlet streams, and final buffer pH and conductivity	Final buffer composition, pH and conductivity	<ul style="list-style-type: none"> <li>• Substantial reduction in buffer storage requirements thereby reducing inventory, capital and cleaning costs</li> <li>• Buffer preparation is simplified reducing labour requirements</li> <li>• Shorter buffer preparation times</li> <li>• Single component concentrates have longer shelf-life than final buffer solution</li> <li>• Reduced risk of waste buffer</li> </ul>	<ul style="list-style-type: none"> <li>• Requires at least 4 inlets, each with its own pump, valves and controls</li> <li>• Feedback control results in consumption of additional buffer until a stable pH and/or conductivity is obtained (~1 min to obtain stable conditions)</li> <li>• Novelty of the system and consumption of buffer as it is produced introduces more regulatory considerations</li> </ul>	[29,33]

- 
- Can be used to facilitate controlled gradient elution
  - Feedback control improves robustness by reducing buffer variability
  - Additional validation and maintenance costs introduced
- 

1471

1472

1473 **Table 3.** Summary of chromatography process control strategies in research and process development.

Equipment	Location	Attribute Measured and Model Implemented	Process Variable(s) Controlled	Benefits	Issues	References
UV Spectrophotometer	Column outlet OR Column outlet and inlet	Protein concentration • Single UV-wavelength model	• Column switching • Product fractionation times	<ul style="list-style-type: none"> <li>• Column switching and fractionation dictated by product breakthrough</li> <li>• No time-based performance decline after 31 days and 160 cycles of continuous operation</li> <li>• Can handle high feed concentrations (&gt;30 g/L)</li> <li>• Control independent of the cell culture feedstock and titer</li> </ul>	<ul style="list-style-type: none"> <li>• Increased implementation and operational complexity</li> <li>• Single wavelength absorbance cannot differentiate between product and impurity</li> </ul>	[40,56,57]
	Column outlet	Protein concentration • Multi-wavelength PLS model	• Product fractionation times	<ul style="list-style-type: none"> <li>• Differentiates product and impurities by utilizing UV-spectra rather than single wavelength during loading</li> <li>• Improved product purity and yields</li> </ul>	<ul style="list-style-type: none"> <li>• Challenges related to the scale up, robustness of the method, and the optimization of the measurement time</li> <li>• Accuracy of model suffers as number of impurities increases</li> </ul>	[60]
	Column inlet and outlet	Protein concentration • Single UV-wavelength model fed into mechanistic model	• Column switching • Product fractionation times	<ul style="list-style-type: none"> <li>• Model accounts for variation in feed</li> <li>• Column switching and fractionation dictated by product breakthrough</li> <li>• 2.5-fold higher capacity utilization</li> </ul>	<ul style="list-style-type: none"> <li>• Low concentration ranges utilized (0.2-0.8 g/L)</li> <li>• Model may not capture all variability present in the system</li> </ul>	[61]
Variable pathlength UV-vis Spectrophotometer	Column outlet AND/OR inlet	Protein concentration • Single UV-wavelength or multi-wavelength PLS model	• Column switching • Product fractionation times	<ul style="list-style-type: none"> <li>• Accurate measurements over a large concentration range (&lt;80 g/L)</li> <li>• Differentiates product and impurities</li> <li>• Column switching and fractionation dictated by predicted protein concentrations</li> </ul>	<ul style="list-style-type: none"> <li>• Large measurement time (~30s)</li> <li>• Single wavelength absorbance cannot differentiate between product and impurity</li> </ul>	[22,77]
Near Infrared Spectrophotometer	Column inlet and outlet	Protein concentration • Multi-wavelength PLS model	• Column switching • Product fractionation times	<ul style="list-style-type: none"> <li>• Rapid measurements (3s)</li> <li>• High accuracy and precision of mAb quantification</li> <li>• Column switching and fractionation dictated by inlet concentration and predicted protein concentration</li> </ul>	<ul style="list-style-type: none"> <li>• Has currently not been scaled up for industrial scale</li> </ul>	[62]
Multi-angle light scattering (MALS)	Column Outlet	Protein aggregate levels • MALS/UV dual model	• Product fractionation times	<ul style="list-style-type: none"> <li>• Rapid measurements (&lt;1s)</li> <li>• Reduces and controls aggregate levels in fractions</li> <li>• Removes the need for post purification analysis</li> </ul>	<ul style="list-style-type: none"> <li>• Rapid changes in concentration may affect MALS accuracy</li> <li>• May be challenging to implement in other unit operations with significant difference in</li> </ul>	[22,76]

					matrices and buffer conductivities. <i>E.g</i> bind-and-elute chromatography	
Tryptophan Fluorescence Spectrophotometer	In-column	Monitoring and control of resin fouling • Single-wavelength fluorescence model	• CIP	<ul style="list-style-type: none"> <li>• Predicts critical fouling levels</li> <li>• Improves column lifespan</li> <li>• Optimizes CIP buffer utilization</li> <li>• No significant loss of yield observed after 200 cycles</li> </ul>	<ul style="list-style-type: none"> <li>• Only determines column fouling and must be combined with other PATs/control methods</li> <li>• Single wavelength utilization limits the accuracy of the PAT</li> </ul>	[65,66]
Attenuated Total Reflection-Fourier Transform Infrared (ATR-FTIR) Spectrophotometer	In-column	Monitoring and control of resin fouling • Multi-wavelength PLS model	• CIP	<ul style="list-style-type: none"> <li>• Predicts critical fouling levels</li> <li>• Improves column lifespan</li> <li>• Optimizes CIP buffer utilization</li> <li>• Spectra based PLS model</li> </ul>	<ul style="list-style-type: none"> <li>• Only determines column fouling and must be combined with other PATs/control methods</li> <li>• Further scale-up studies are required.</li> </ul>	[63]

1474